

## ARTICLE

# Histological analysis of ankylothecondonty in Silesauridae (Archosauria: Dinosauriformes) and its implications for the evolution of dinosaur tooth attachment

Gabriel Mestriner<sup>1</sup>  | Aaron LeBlanc<sup>2,3</sup>  | Sterling J. Nesbitt<sup>4</sup>  |  
 Júlio C. A. Marsola<sup>1,5</sup>  | Randall B. Irmis<sup>6</sup> | Átila Augusto Stock Da-Rosa<sup>7</sup>  |  
 Ana Maria Ribeiro<sup>8</sup> | Jorge Ferigolo<sup>8</sup> | Max Langer<sup>1</sup> 

<sup>1</sup>Departamento de Biologia, Universidade de São Paulo, Ribeirão Preto, Brazil

<sup>2</sup>Department of Biological Sciences, University of Alberta, Edmonton, Alberta, Canada

<sup>3</sup>Faculty of Dentistry, Oral, & Craniofacial Sciences, King's College London, London, UK

<sup>4</sup>Department of Geosciences, Virginia Tech, Blacksburg, Virginia

<sup>5</sup>Programa de Pós-Graduação em Biologia Animal, Instituto de Biociências, Letras e Ciências Exatas, UNESP Campus de São José do Rio Preto, São Paulo, Brazil

<sup>6</sup>Natural History Museum of Utah and Department of Geology & Geophysics, University of Utah, Salt Lake City, Utah

<sup>7</sup>Laboratório de Estratigrafia e Paleobiologia, Departamento de Geociências, Universidade Federal de Santa Maria, Santa Maria, Rio Grande do Sul, Brazil

<sup>8</sup>Museu de Ciências Naturais, Secretaria do Meio Ambiente e Infraestrutura, Porto Alegre, RS, Brazil

## Correspondence

Gabriel Mestriner, Departamento de Biologia, Universidade de São Paulo, Avenida Bandeirantes 3900, Ribeirão Preto 14040-190, Brazil.  
 Email: gabriel.mestriner93@gmail.com

## Funding information

Center for Hierarchical Manufacturing, National Science Foundation, Grant/Award Numbers: 1349650, 1349667; Coordenação de Aperfeiçoamento de Pessoal de Nível Superior, Grant/Award Number: 88887468538/2019-00; Fundação

## Abstract

Dinosaurs possess a form of tooth attachment wherein an unmineralized periodontal ligament suspends each tooth within a socket, similar to the condition in mammals and crocodylians. However, little information is known about tooth attachment and implantation in their close relatives, the silesaurids. We conducted a histological survey of several silesaurid taxa to determine the nature of tooth attachment in this phylogenetically and paleoecologically important group of archosaurs. Our histological data demonstrate that these early dinosauriforms do not exhibit the crocodylian/dinosaur condition of a permanent gomphosis, nor the rapid ankylosis that is plesiomorphic for amniotes. Instead, all sampled silesaurids exhibit delayed ankylosis, a condition in which teeth pass through a prolonged stage where the teeth are suspended in sockets by a periodontal ligament, followed by eventual mineralization and fusion of the tooth to the jaws. This suggests that tooth attachment in crocodylians and dinosaurs represent the further retention of an early ontogenetic stage compared to silesaurids, a paedomorphic trend that is mirrored in the evolution of synapsid tooth attachment. It also suggests that the dinosaur and crocodylian gomphosis was convergently acquired via heterochrony or, less likely, that the silesaurid condition represents a reversal to a plesiomorphic state. Moreover, if Silesauridae is nested within Ornithischia, a permanent gomphosis could be convergent between the two main dinosaur lineages, Ornithischia and Saurischia. These results demonstrate that dental characters in early archosaur phylogenies must be chosen and defined carefully, taking into account the relative duration of the different phases of dental ontogeny.

## KEYWORDS

alveolar bone, cementum, dental histology, heterochrony, ontogeny, periodontal ligament, Sharpey fibers

de Amparo à Pesquisa do Estado de São Paulo, Grant/Award Numbers: 2018/24031-6, 2019/07510-0

## 1 | INTRODUCTION

Comparative dental anatomy is a pivotal area of study in vertebrate evolution (Wang et al., 2015). Because tooth shape is often tied to diet, teeth provide crucial data for interpreting feeding ecology of extinct and extant organisms (e.g., Brink et al., 2015; Hendrichx, Mateus, & Araújo, 2015; Melstrom & Irmis, 2019). One aspect with important evolutionary implications is the histological study of tooth attachment and implantation (LeBlanc, Brink, Cullen, & Reisz, 2017; LeBlanc & Reisz, 2013). Evolutionary changes in these features have yielded valuable insights into the paleoecology and palaeobiology of numerous amniote clades (Caldwell, Budney, & Lamoureux, 2003; LeBlanc et al., 2017; LeBlanc, Brink, Whitney, Abdala, & Reisz, 2018; Pretto, Cabreira, & Schultz, 2014; Zaher & Rieppel, 1999).

The study of tooth implantation and attachment in key extinct taxa helped unveil evolutionary transitions in major tetrapod groups, such as the origin of the ligament-based tooth attachment (gomphosis) in Mammalia, which can be traced deep down the stem of this lineage among Permo-Triassic synapsids (LeBlanc et al., 2018). Such investigations examine two distinct aspects of dental anatomy: (a) tooth implantation, which categorizes teeth by their spatial relations within the jaws; (b) tooth attachment, which distinguishes those that are fused to the jaw (ankylosis) from those anchored by a periodontal ligament (gomphosis) (Bertin, Thivichon-Prince, LeBlanc, Caldwell, & Viriot, 2018; Budney, Caldwell, & Albino, 2006; Caldwell, 2007; Caldwell et al., 2003; LeBlanc et al., 2017). Mammals and crocodylians have received considerable attention, because of their seemingly unique combination of thecodont implantation (teeth deeply implanted in the jaws) and permanent gomphosis (LeBlanc et al., 2017). Traditionally, mammals and crocodylians are interpreted as possessing an “advanced” (apomorphic) condition, with associated attachment tissues (i.e., cellular cementum, alveolar bone, and periodontal ligament) that evolved independently in both groups. However, more recent evaluations of several fossil taxa revealed that those three tooth attachment tissues are present ancestrally in all major amniote clades (Budney et al., 2006; Caldwell et al., 2003; Dumont et al., 2016; García & Zurriaguz, 2016; LeBlanc et al., 2017, 2018; LeBlanc & Reisz, 2013; Maxwell, Caldwell, & Lamoureux, 2011; Pretto et al., 2014; Sassoon, Foffa, & Marek, 2015).

Distinguishing tooth attachment from tooth implantation is crucial for understanding how these aspects are related and what they reveal about dental evolution in amniotes (LeBlanc et al., 2017). Traditionally, the tissue that fuses most reptile teeth to the jaws was considered non-homologous to the attachment tissues of mammals (Kearney & Rieppel, 2006; Peyer, 1968; Tomes, 1874). The emerging alternative interpretation is that teeth fuse to the jaws when the alveolar bone, forming the socket, and the cellular cementum, coating the roots, contact one another completely, leaving no space for the periodontal ligament around the tooth root (LeBlanc, Reisz, Brink, & Abdala, 2016). The presence of extensive Sharpey's fiber networks in the hard tissues surrounding ankylosed teeth has revealed that the so-called “bone of attachment” (sensu Tomes, 1874) in fact encompasses the three attachment tissues observed in mammals. The Sharpey's fiber networks in the hard tissues surrounding ankylosed teeth must have been the insertion points of a periodontal ligament that was completely mineralized during dental ontogeny, and it is worth to mention that, in fossils, its unmineralized portion is completely gone, so that just traces of these structures are left (Caldwell et al., 2003; LeBlanc et al., 2017; LeBlanc et al., 2018; LeBlanc & Reisz, 2013). This alternative view establishes homology between the attachment tissues of all amniotes with either a gomphosis or ankylosis type of tooth attachment, suggesting that the differences between the two are solely related to the developmental timing and the extent of mineralization of the attachment tissues (LeBlanc et al., 2017, 2018). A remaining outstanding question is in which amniote groups these evolutionary changes took place. This has been investigated for early synapsids and mammals, as well as for some squamates, but remains virtually unexplored within Archosauria.

Crocodylians are the only living archosaurs with a permanent gomphosis (Luan et al., 2009; McIntosh et al., 2002; Miller, 1968), but this condition is also present in non-avian dinosaurs (Fong, LeBlanc, Berman, & Reisz, 2016; LeBlanc et al., 2017). As in mammalian tooth attachment, the periodontal ligament remains (partially or completely) non-mineralized, connecting the root cementum to the alveolar bone and occupying a space between them that is retained during the entire tooth ontogeny (Caldwell et al., 2003; Chen, LeBlanc, Jin, Huang, & Reisz, 2018; Fong et al., 2016; García & Zurriaguz, 2016; Kvam, 1960; LeBlanc et al., 2016; LeBlanc et al., 2017; LeBlanc et al., 2018; LeBlanc & Reisz, 2013; Maxwell et al., 2011; McIntosh

et al., 2002; Miller, 1968). However, although the dinosaur and crocodylian gomphosis mode of tooth attachment presumably have a single origin from a common archosaur ancestor (Edmund, 1960; Fong et al., 2016; LeBlanc et al., 2017; LeBlanc et al., 2018; Martz & Small, 2019; Nesbitt et al., 2010), new discoveries suggest that several non-archosaurian archosauromorphs have the so-called ankylothecondont condition (e.g., rhynchosaurs, *Prolacerta*, *Proterosuchus*, *Sarmatosuchus*—Ezcurra, 2016; Nesbitt, 2011).

The ankylothecondont tooth attachment also occurs in early amniotes, as well as in squamates and synapsids, encompassing all of the plesiomorphic amniote tissues (cementum, alveolar bone, and periodontal ligament), but with the periodontal ligament completely mineralized (Caldwell et al., 2003; LeBlanc et al., 2017, 2018; LeBlanc & Reisz, 2013; Luan et al., 2009). Among avian-line archosaurs, silesaurids (Ezcurra, 2016; Ezcurra, Nesbitt, Fiorelli, & Desojo, 2019; Ferigolo & Langer, 2007; Kammerer, Nesbitt, & Shubin, 2011; Langer, Nesbitt, Bittencourt, & Irmis, 2013; Martz & Small, 2019; Nesbitt, 2011; Nesbitt et al., 2010) comprise a key group that can shed light on the evolution of dinosaur tooth attachment, because of their ankylothecondont condition, which has never been examined histologically. Here, we assess this complex feature, providing a comprehensive characterization of silesaurid tooth attachment based on four different members of the group, spanning much of the Triassic Period (Anisian—Norian). Further, we evaluate its evolutionary implications for the diversification of dinosauriforms and the origins of gomphosis in dinosaurs.

Silesaurids have a controversial phylogenetic position among Dinosauriformes; most analyses recover them as the sister-group of Dinosauria (Baron, Norman, & Barrett, 2017; Benton & Walker, 2011; Bittencourt, Arcucci, Marsicano, & Langer, 2015; Langer et al., 2017; Langer, Ezcurra, Bittencourt, & Novas, 2010; Nesbitt, 2011; Nesbitt et al., 2017), but others place them within the ornithischian lineage (Cabeira et al., 2016; Ferigolo & Langer, 2007; Langer & Ferigolo, 2013; Müller & Garcia, 2020). Also, their inferred ankylothecondonty has been suggested as a synapomorphy of a monophyletic Silesauridae (e.g., character 174 of Ezcurra, 2016; Ezcurra et al., 2019; Ferigolo & Langer, 2007; Kammerer et al., 2011; Langer et al., 2013; Martz & Small, 2019; Nesbitt, 2011; Nesbitt et al., 2010; Nesbitt, Langer, & Ezcurra, 2020). In addition to their phylogenetic importance, silesaurids are paleoecologically intriguing because they are the earliest dinosauriform lineage with cranial and dental specializations for an omnivorous and/or herbivorous diet (Langer & Ferigolo, 2013; Nesbitt et al., 2010; Qvarnström et al., 2019). Improving our understanding of

tooth attachment in silesaurids may be therefore pivotal for inferring their relationships and paleoecology, which is itself critical for understanding the origin of dinosaurs and the key-features that promoted their evolutionary success (Benton, Forth, & Langer, 2014; Brusatte et al., 2010; Brusatte, Benton, Ruta, & Lloyd, 2008; Langer et al., 2010; Langer et al., 2013).

## 1.1 | Institutional abbreviations

**MCN**, Museu de Ciências Naturais, Secretaria do Meio Ambiente e Infraestrutura, Porto Alegre, Brazil; **NMT**, National Museum of Tanzania, Dar es Salam, Tanzania; **UFSM**, Universidade Federal de Santa Maria, Rio Grande do Sul, Brazil.

## 2 | MATERIALS AND METHODS

### 2.1 | Specimens

This study is based on histological transverse sections of tooth-bearing bones of four silesaurids: 1—the Hayden Quarry silesaurid (GR 1072), most likely referable to *Eucoelophysis baldwini*, from the Petrified Forest Member of the Chinle Formation, late Norian of New Mexico, USA (Breedon, Irmis, Nesbitt, Smith, & Turner, 2017; Ezcurra, 2006; Irmis et al., 2007; Sullivan & Lucas, 1999); 2—*Sacisaurus agudoensis* (MCN PV 10095) from the Caturrita Formation, early Norian of Brazil (Ferigolo & Langer, 2007; Marsola et al., 2018); 3—*Asilisaurus kongwe* (NMT RB 1086; NMT RB 1087) from the Lifua Member of the Manda Beds, Middle Triassic of Tanzania (Nesbitt et al., 2010; Nesbitt et al., 2017; Peacock, Steyer, Tabor, & Smith, 2018); 4—UFSM 11579, a newly recovered silesaurid (Mestriner, Marsola, DaRosa, & Langer, 2018) from the upper Alemoa Member of the Santa Maria Formation at Cerro da Alemoa, late Carnian of Brazil (Langer, Ramezani, & Da Rosa, 2018). All measurements taken for the specimens are available in Table 1. The lack of anterior and posterior ends of all specimens (except for NMT RB 1086) hampers inferring the anatomical position of each tooth and/or alveolus, so the numbers ascribed to them in the sections below serve only for descriptive purposes.

### 2.2 | Methods

The specimens were prepared and analyzed at the palaeo histology lab at the University of Alberta (Edmonton, Canada). Molds and casts were made prior to thin sectioning. Moulds were made using Blustar Silicones V-SIL

TABLE 1 Measurements taken from the specimens

Specimen/osteohistology information	GD ( $\mu\text{m}$ )	AC ( $\mu\text{m}$ )	CC ( $\mu\text{m}$ )	AB ( $\mu\text{m}$ )	JB ( $\mu\text{m}$ )
Hayden Quarry silesaurid (GR 1072)	24	10	114	500	750
UFSM 11579—maxilla	20	13	100	300	290
UFSM 11579—dentary	20	11	91	370	125
<i>Sacisaurus agudoensis</i>	NA	9	57	145	142
<i>Asilisaurus konwge</i> 1086	18	10	57	227	227
<i>Asilisaurus kongwe</i> 1087	18	10	91	182	409

Abbreviations: AB, alveolar bone; AC, acellular cementum; CC, cellular cementum; GD, globular dentine; JB, jaw bone.

1062 and Hi Pro Green catalyst, and casts by pouring Smooth-On-Smooth-Cast 321 or 322 liquid plastic into the silicon molds and placing them under pressure until they set (LeBlanc et al., 2018). All paleohistological sections followed the standard procedures employed for sectioning fossil material according to LeBlanc et al. (2018). The specimens were separately fully embedded in *Castolite AC* polyester resin in a plastic container and then peroxide catalyst was incorporated in a ratio of 10 methyl ethyl ketone peroxide drops for 30 mL of resin. Then, the specimens were vacuumed for 5 min to evacuate all air bubbles, and left to set for 24 hr.

The embedded specimens were cut using a *Buehler Isomet 1000* water blade saw set to a speed of 200–300 rpm (revolutions per minute). After cutting, the surfaces were polished using 600 and 1,000 grit silicon carbide powder suspensions. After polishing, they were left to dry for 24 hr and mounted to plexiglass frosted slides using *Scotch-Weld SF-100* cyanoacrylate glue to stick the specimens to the slide. Once fixed, the thick sections were cut using the *Isomet 1000* at a trim thickness of approximately 0.7 mm. The specimens were then ground down using the *Hillquist* grinding machine. The sections were constantly checked under the microscope until they nearly reached the desired optical clarity. Once the slide was nearing the desired thickness, the final grinding was done by hand with 600 and 1,000-grit silicon carbide powder and a glass plate. The specimens were then polished with 1- $\mu\text{m}$  aluminum oxide powder and a soft cloth.

Images of the thin sections were taken using a *Nikon DS-f3* camera mounted to a *Nikon E600 POL* microscope using *Nikon NIS-Elements* imaging software. All the measurements in Table 1 were taken by manually scaling and measuring randomly five different spots of each tissue or structure of interest and averaging their values. The identification, delimitation, and measurements of the periodontal tissues followed previous histological surveys for fossil and extant animals (quoted throughout the text). The original slides and remaining embedded specimens are available at the following institutions: NMT RB 1086, NMT RB 1087 (*A. kongwe*)—currently housed Department of

Geosciences, Virginia Tech, Blacksburg, VA; GR 1072 (Hayden silesaurid)—Ruth Hall Museum of Paleontology at Ghost Ranch, NM; MCN PV 10095 (*S. agudoensis*)—Museu de Ciências Naturais, Secretaria do Meio Ambiente e Infraestrutura, Porto Alegre-RS, Brazil; UFSM 11579—Departamento de Geociências, Universidade Federal de Santa Maria, Santa Maria-RS, Brazil.

### 3 | RESULTS

We identified the tooth attachment tissues based on their characterization in previous studies (Bertin et al., 2018; Caldwell et al., 2003; Chen et al., 2018; Fong et al., 2016; LeBlanc & Reisz, 2013; LeBlanc et al., 2017, 2018; LeBlanc, Paparella, Lamoureux, Doschak, & Caldwell, 2020; Nanci, 2013). The tooth socket is formed by alveolar bone, which is a vascularized bone tissue, with a matrix typically comprising dense Haversian bone in mammals (in which the alveolar bone may also contain lamellar bone in addition to dense Haversian bone; Nanci, 2013), and woven-fiber matrix in most other amniotes (Caldwell et al., 2003; LeBlanc et al., 2017, 2018; LeBlanc & Reisz, 2013; Nanci, 2013). The tooth root is coated in cementum (which can be cellular or acellular), providing an attachment area for the periodontal ligament, which is also anchored to the alveolar bone that forms the tooth socket (LeBlanc & Reisz, 2013). The periodontal ligament comprises an unmineralized network of collagen fibers, and serves multiple purposes, such as providing a flexible attachment for the tooth to the alveolar bone, facilitating post-eruptive tooth movement, and a sensory system to help in proper positioning of the jaws during mastication (Nanci, 2013).

#### 3.1 | Hayden Quarry silesaurid

The sampled bone is a right dentary fragment (GR 1072—Figure S1). Its anterior and posterior edges are damaged, but tooth implantation is well-preserved (Figures 1–4). The fragment preserves eight alveoli; the

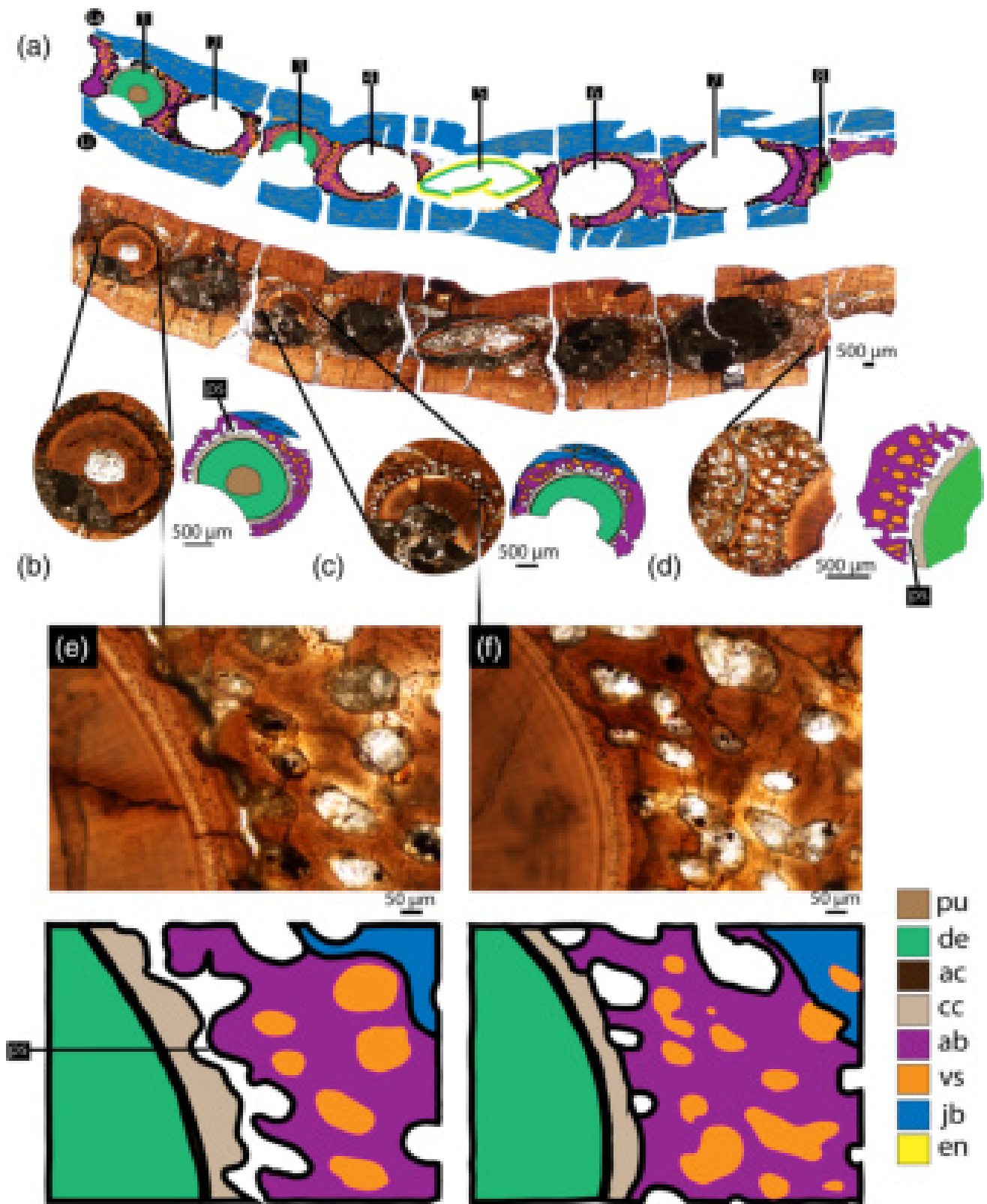


**FIGURE 1** Hayden Quarry silesaurid (GR 1072) right dentary, dental tissues in transverse section at root level, with diagrammatic illustrations. (a) General view. (b)–(d) Teeth of the first, third, and eighth alveoli. (e) Detail of “b,” showing unmineralized periodontal space. (f) Detail of “c” showing the contact between alveolar bone and cellular cementum. ac = acellular cementum; ab = alveolar bone; cc = cellular cementum; de = dentine; en = enamel; jb = jaw bone; La = labial side; Li = lingual side; ps = periodontal space; pu = pulp cavity; vs = vascular spaces. Numbers indicate alveoli position

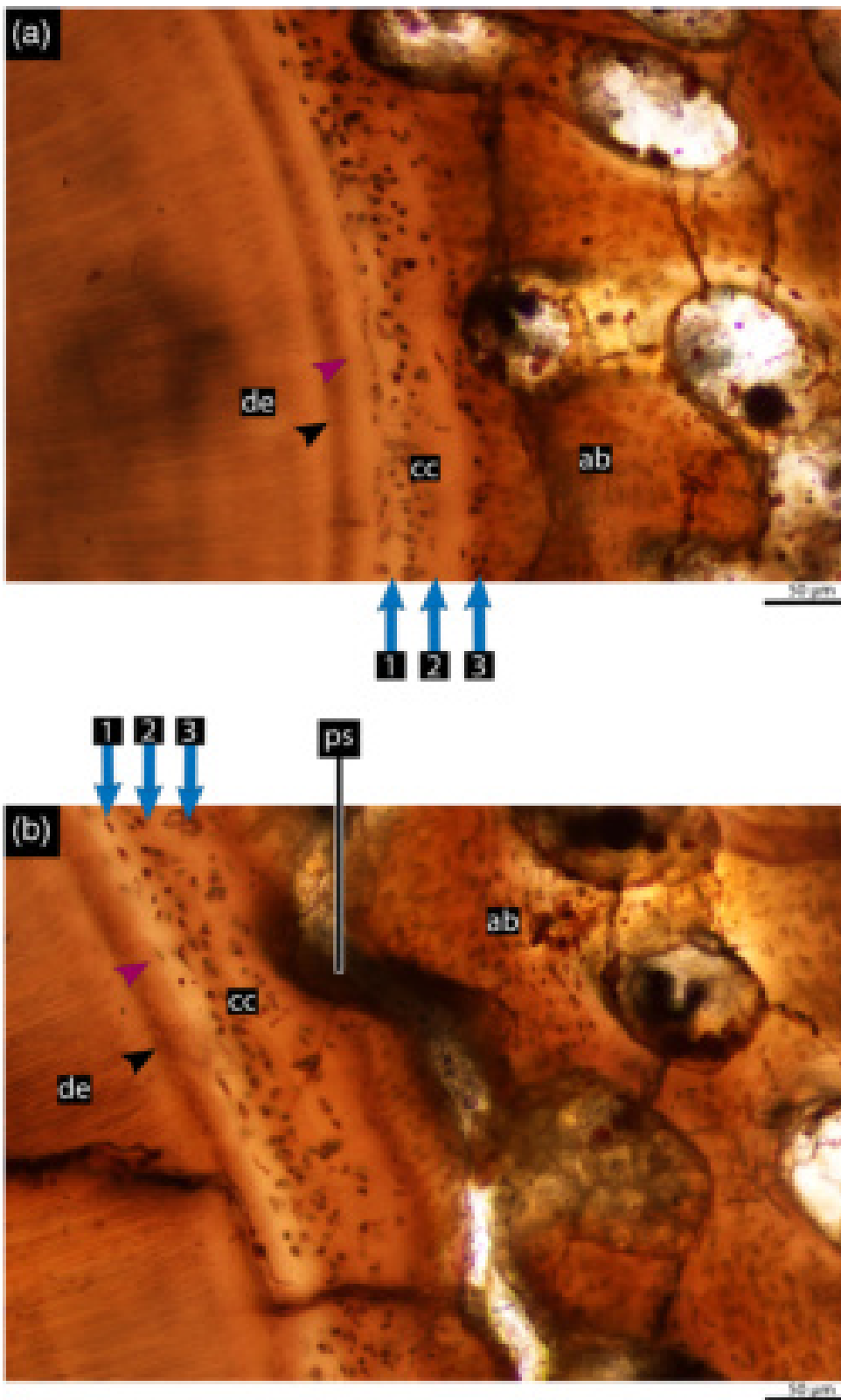


**FIGURE 2** Hayden Quarry silesaurid (GR 1072) right dentary, dental tissues in transverse section at root level. (a) Detail of the tooth in the third alveolus, showing the contact between cellular cementum and alveolar bone (mineralized periodontal space). (b) Detail of the tooth in the first alveolus, showing unmineralized periodontal space. ab = alveolar bone; cc = cellular cementum; de = dentine; ps = periodontal space. Black arrow indicates the layer of globular dentine, blue arrows indicate first, second, and third layers of cellular cementum, purple arrow indicates the acellular cementum

first, third, and eighth of which contain fully erupted tooth crowns (Figure 1a). Additionally, a replacement tooth is emerging from the fifth alveolus. The crown in the eighth alveolus has only its anteriormost portion preserved. Alveoli 2, 4, 6, and 7 are empty. Due to

taphonomic distortions, the bone is arched laterally. This specimen was serially sectioned three times across the whole dentary.

**Histology:** As in all amniotes, dentine forms the bulk of the teeth, with dental tubules extending across their

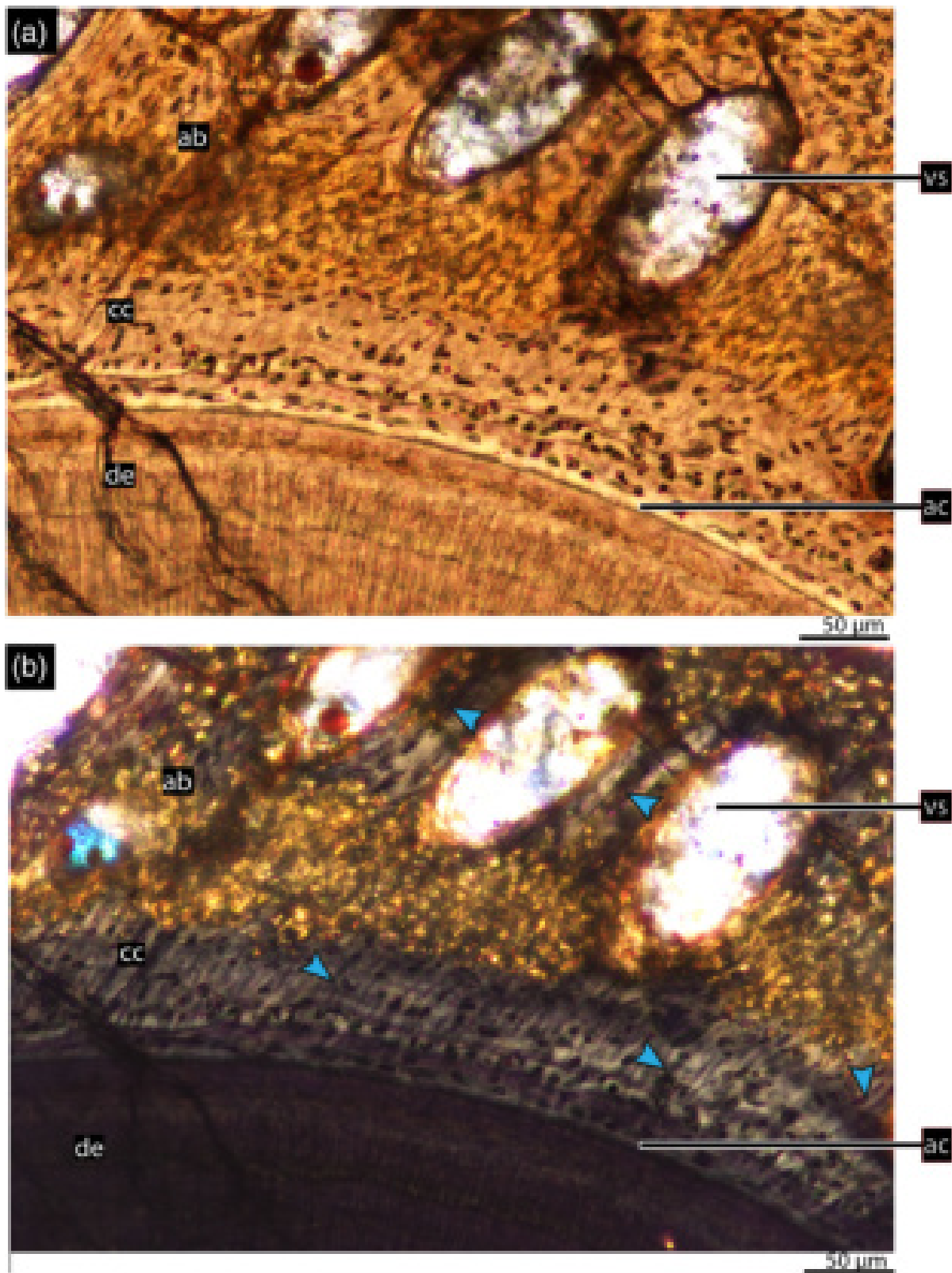


**FIGURE 3** Hayden Quarry silesaurid (GR 1072) right dentary, dental tissues in transverse section at root level. (a) Details of the tooth positioned in the third alveolus, showing the alveolar bone and cellular cementum contact and a periodontal space completely mineralized. (b) “a” under cross-polarized light, showing Sharpey’s fibers across the cellular cementum and alveolar bone layers (blue arrows). ac = acellular cementum; ab = alveolar bone; cc = cellular cementum; de = dentine; vs = vascular spaces

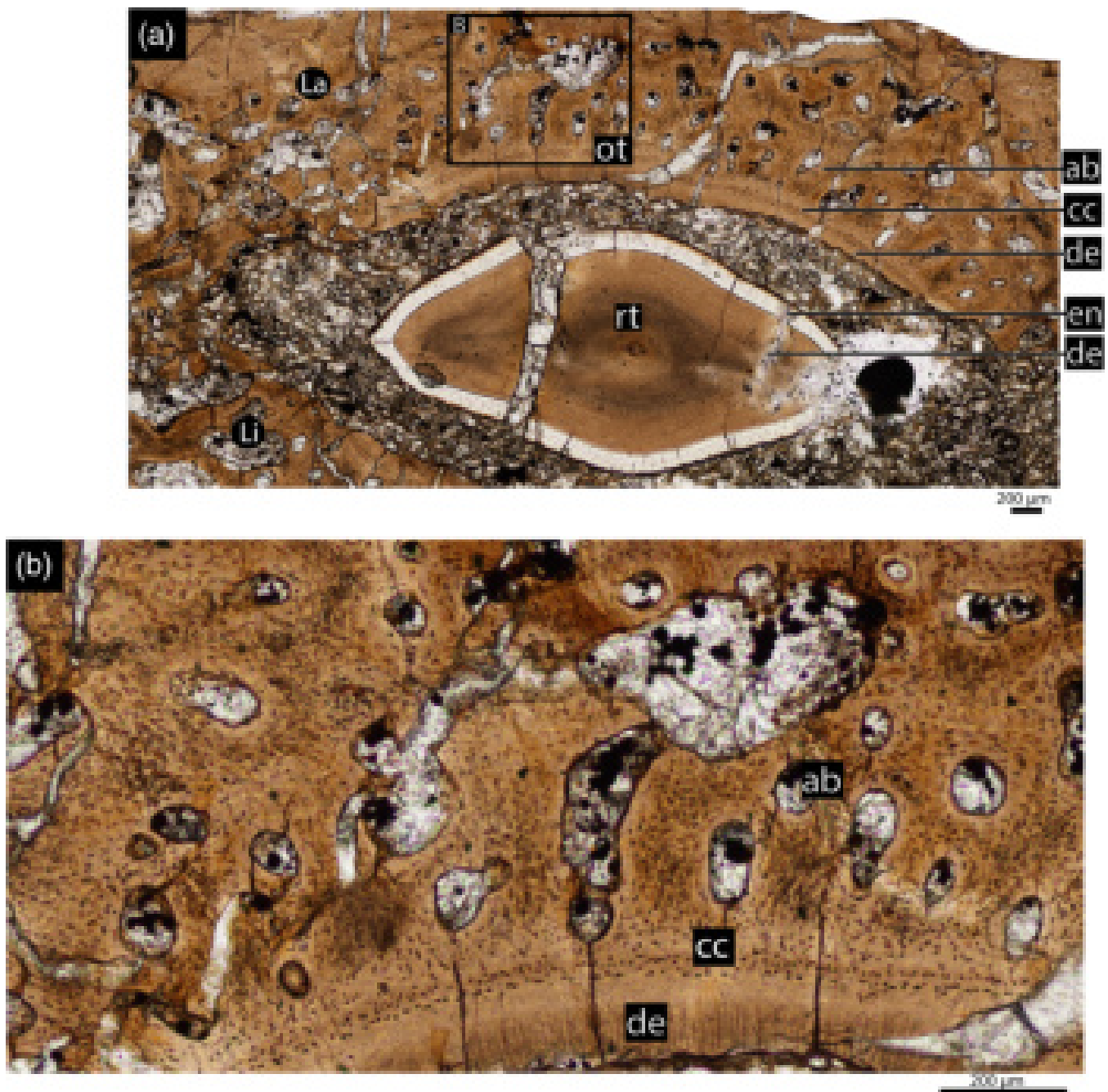


**FIGURE 4** Hayden Quarry silesaurid (GR 1072) right dentary, dental tissues in transverse section at root level. Replacement tooth and old tooth generation (fifth alveolus). (a) Replacement tooth and remnant of previous tooth generation. (b) Old tooth generation showing tooth attachment details. Note the contact between cellular cementum and alveolar bone, completely mineralizing the periodontal space (ankylosis). ab = alveolar bone; cc = cellular cementum; de = dentine; en = enamel; La = labial side; Li = lingual side; ot = old tooth generation; rt = replacement tooth

entire thickness. The roots of all functional teeth (first, third, and eighth alveoli—Figure 1a–d) show a dark layer of globular dentine (ca. 24 µm) along the outer margins, separating the orthodentine from the root cementum (Figure 2). The globular dentine is a zone of initial dentine formation and is poorly mineralized. This layer corresponds to the granular layer of Tomes (Fong

et al., 2016; Nanci, 2013). This is similar to the condition observed in other tetrapods, including the neotheropod dinosaur *Coelophysis bauri* (Fong et al., 2016; LeBlanc & Reisz, 2013).

The acellular cementum is a clear, featureless band external to the globular dentine (Figure 2) and is thinner than the globular dentine (ca. 10 µm). The cellular

cementum is much thicker than the acellular layer (ca. 114  $\mu\text{m}$ ; Figures 2 and 3). It contains randomly distributed cementocyte lacunae, which are oval to circular. The cellular cementum also contains incremental growth bands that are roughly parallel to the external surface of the dentine (Figure 2). The innermost layer of cellular cementum is the lightest in color, whereas the external layers are the darkest. Sharpey's fibers perforate the cellular cementum perpendicularly, radiating around the circumference of the root. These fibers are better seen under cross-polarized light (Figure 3b), where it is possible to identify their bundles radiating within the cellular cementum, extending towards the alveolar bone and the tooth roots.

The teeth in the first and eighth alveoli (Figures 1b,d, e and 2b) show periodontal spaces (ca. 56  $\mu\text{m}$  thick) between the cellular cementum and the alveolar bone, indicating that the teeth were attached by soft tissue in life (a gomphosis, sensu Fong et al., 2016; LeBlanc et al., 2017, 2018). The inner and outer margins of the periodontal space are uneven and sinuous around the root circumference, due to the presence of partially enclosed vascular spaces. In this arrangement, the vascular spaces are located at the intersections between the alveolar bone and cellular cementum (Figures 1e and 2b). The tooth in the third alveolus is ankylosed to the jaw (Figure 1c,f), meaning that the periodontal space is absent, with the cellular cementum and the alveolar bone contacting one another (Figures 1f, 2a and 3). In this case, the vascular spaces are mostly displaced to the alveolar bone area, with a minor portion occupying the cellular cementum layer.

The alveolar bone is vascularized along its entire thickness, in all parts of the dentary (ca. 500  $\mu\text{m}$  from tooth root to surrounding bone of the jawbone). The cross section of the vascular space is rounded, indicating that the blood vessels were dorsoventrally directed. The area around some of these vascular spaces is surrounded by lamellar bone, formed by organized cells (Figure 4b; LeBlanc & Reisz, 2013; LeBlanc et al., 2017; Reid, 1996). As expected for archosaurs (LeBlanc et al., 2017), the matrix of the alveolar bone comprises woven bone.

The area between each alveolus (i.e., the interdental bone of LeBlanc et al., 2017), is formed entirely by alveolar bone (Figure S2). The boundary between the alveolar bone of each of the adjacent alveoli is outlined by a reversal line; as is clear in the alveolar bone between the third and fourth alveoli (Figure S2A). The boundary between the alveolar bone and the jawbone is also outlined by a reversal line (Figure S3), indicating that the alveolar bone is resorbed and redeposited (Snyder, LeBlanc, Jun, Bevit, & Reisz, 2020). This line marks the farthest extent of bone resorption and subsequent redeposition of alveolar

bone, between successive tooth replacement cycles (Fong et al., 2016).

The jawbone (ca. 750  $\mu\text{m}$  from the alveolar bone to the outer dentary surface) consists of parallel-fibered bone, in which the cells are flat, organized in rows, and anteroposteriorly arranged. The jawbone and the alveolar bone can easily be distinguished from one another by their different birefringence patterns under cross-polarized light: the jaw bone alternates between dark and bright regions depending on the orientations of the bone matrix, whereas the alveolar bone remains dark, due to its more disorganized crystallite matrix (Figure S3B). Mineral inclusions within the alveolar bone create random bright spots under cross-polarized light within the alveolar bone; however, these appear to be diagenetic features. The primary vascular channels of the jawbone are anteroposteriorly long and mediolaterally thin (Figure 1a; Figure S3).

The teeth of alveoli 1 and 3 show different forms of tooth attachment (Figures 1 and 2). The tooth of alveolus 3 has a periodontal space that is totally mineralized around the root in the two more apical cross sections (-Figure S4A,B), but it has points in which the periodontal space is not mineralized in the more basal section (-Figure S4C). Conversely, the tooth of alveolus 1 has an unmineralized periodontal space, as observed around the entire root in two more apical cross sections (Figure S5A, B), whereas the most basal section reveals some points where the periodontal space is being mineralized by the alveolar bone (Figure S5C).

The dentary has four empty alveoli (positions 2, 4, 6, and 7; Figure 1a). The second, fourth, and sixth are ovoid and not taphonomically deformed. The seventh has the same anteroposteriorly elongated outline also seen in the fifth alveolus, being anteroposteriorly longer (ca. 5 mm) than the other alveoli (ca. 2.5 mm). The replacement tooth erupting from the fifth alveolus (Figures 1a and 4a) has a thin enamel layer. The most apical cross section shows a remaining piece of the replaced tooth, which was not totally resorbed, surrounding the new tooth labially. The attachment tissues of that piece are intact, revealing that the functional tooth was fully ankylosed prior to being replaced (Figure 4b).

### 3.2 | Santa Maria Formation silesaurid—UFSM 11579

The sampled elements correspond to two jaw elements, a left maxilla and a right dentary (Figures 5–9). The maxilla contains four alveoli (Figure 5; Figure S6). The anterior and posterior edges are lost, but the piece is generally well preserved. The fully erupted crowns fill

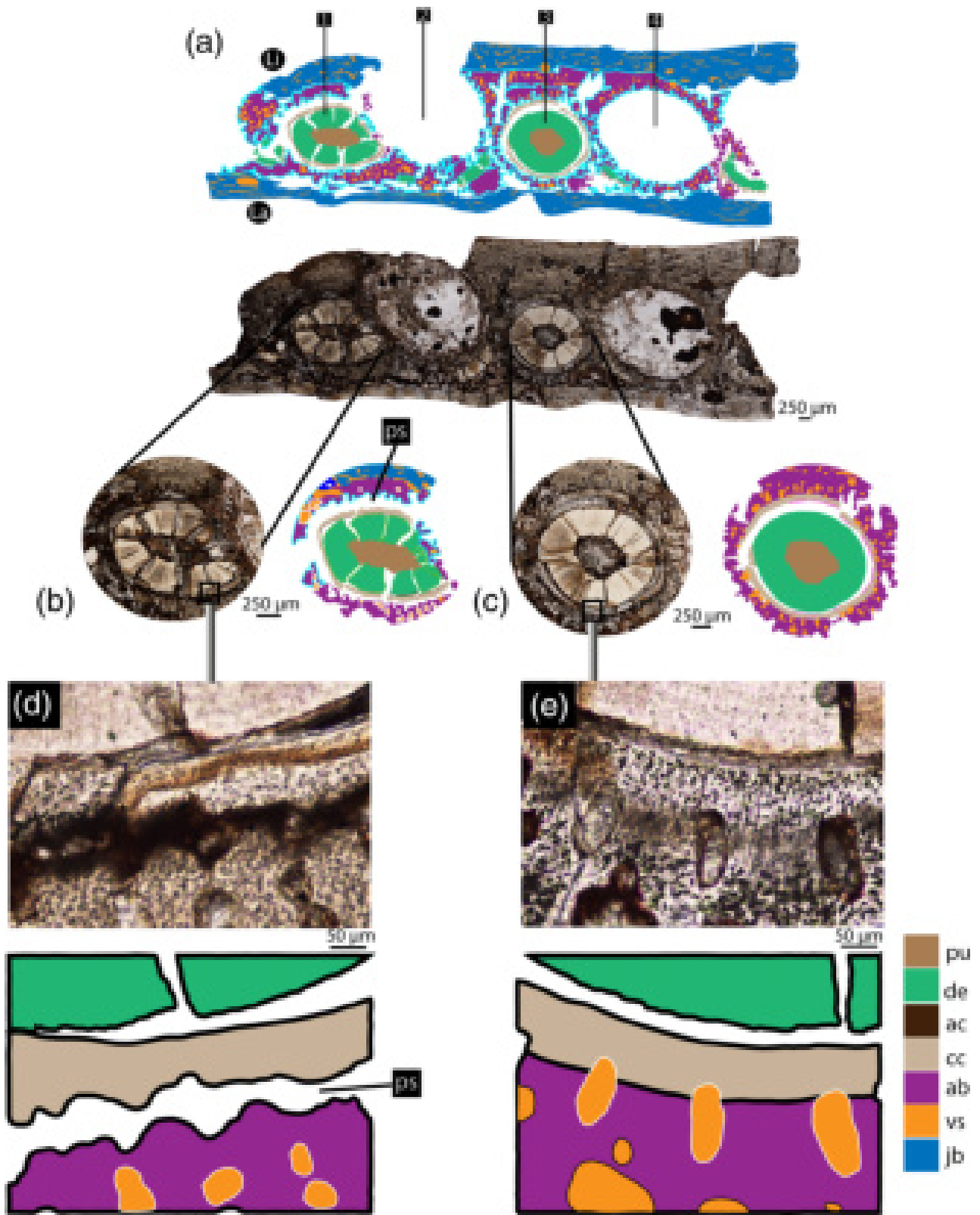


**FIGURE 5** UFSM 11579 left maxilla, dental tissues in transverse section at root level, with diagrammatic illustrations. (a) General view. (b,c) Teeth of the first and third alveoli. (d) Detail of “b,” showing unmineralized periodontal space. (e) Detail of “c” showing the contact between alveolar bone and cellular cementum. ac = acellular cementum; ab = alveolar bone; cc = cellular cementum; de = dentine; jb = jaw bone; La = labial side; Li = lingual side; ps = periodontal space; pu = pulp cavity; vs = vascular spaces

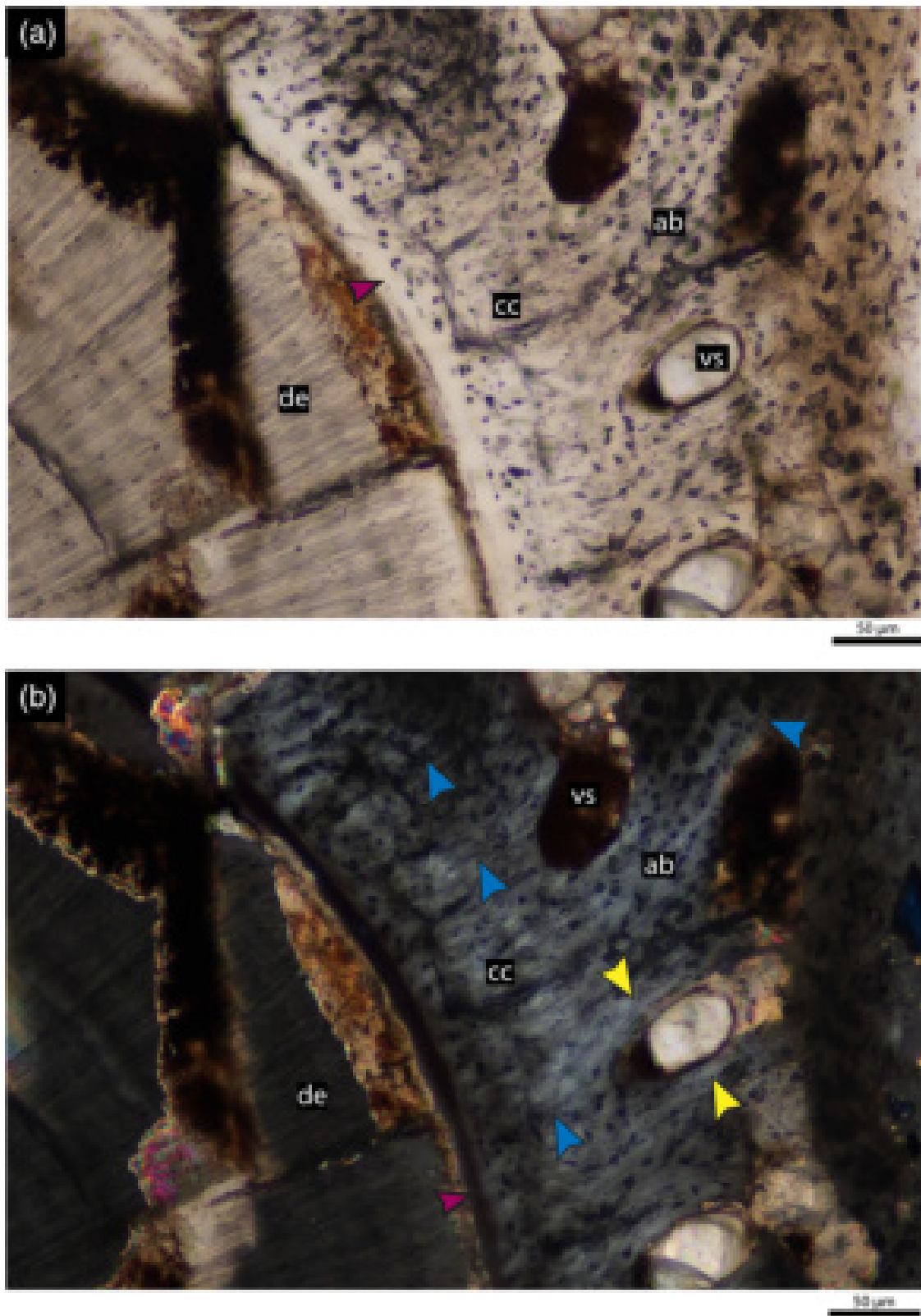


**FIGURE 6** UFSM 11579 left maxilla, dental tissues in transverse section at root level. (a) Details of the tooth positioned in the third alveolus, showing the alveolar bone and cellular cementum contact (mineralized periodontal space). (b) “a” under cross-polarized light, showing Sharpey’s fibers (blue arrows) across the cellular cementum and alveolar bone layers. ab = alveolar bone; cc = cellular cementum; de = dentine; vs = vascular spaces. Yellow arrow indicates lamellar bone; purple arrow indicates the acellular cementum

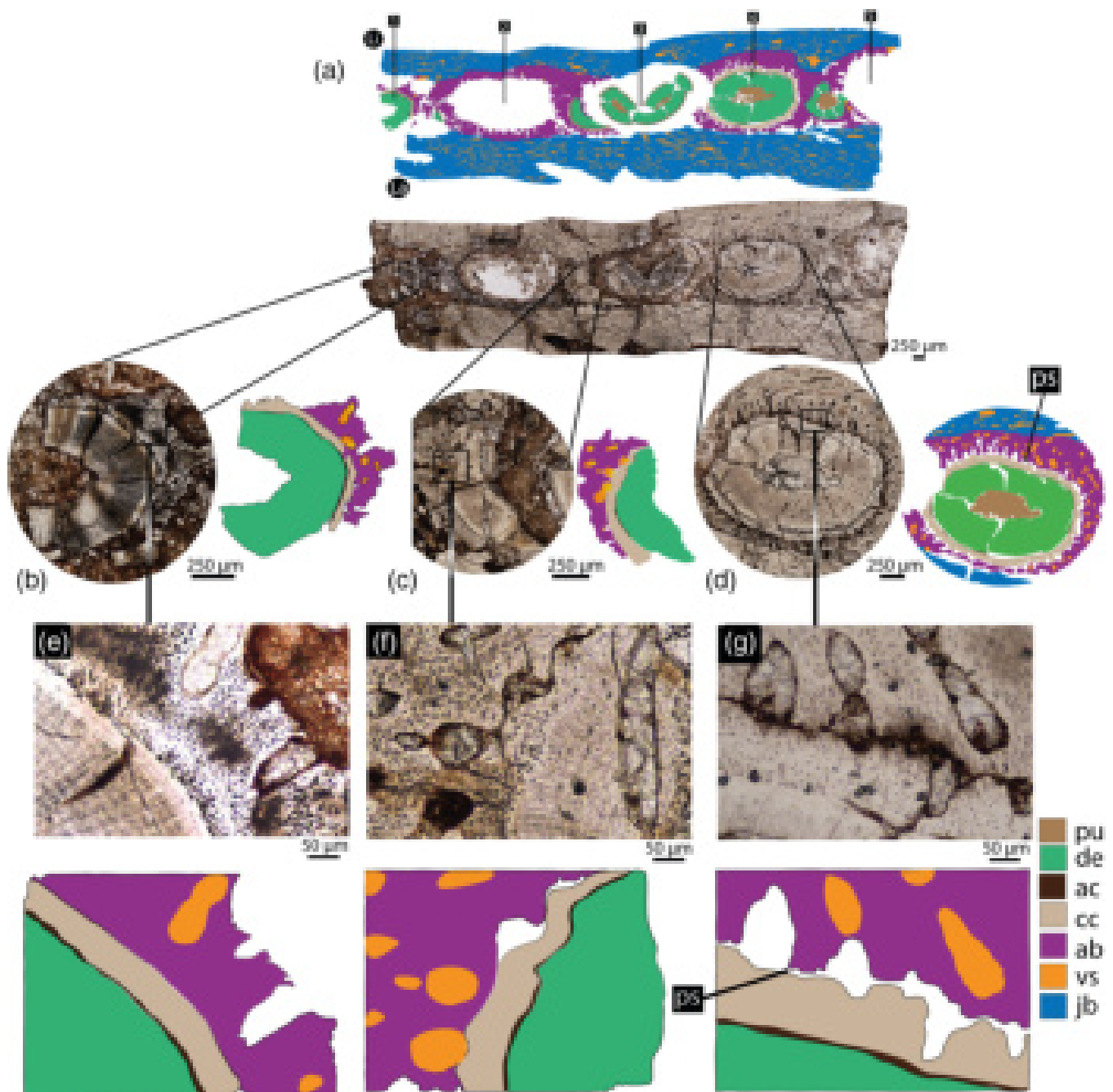


**FIGURE 7** UFSM 11579 right dentary, dental tissues in transverse section at root level, with diagrammatic illustrations. (a) General view. (b) Tooth of the first alveolus. (c) Old generation of tooth of the third alveolus. (d) Tooth of the fourth alveolus. (e, f) Detail of “b” and “c,” showing the contact between alveolar bone and cellular cementum. (g) Detail of “d” showing unmineralized periodontal space. ac = acellular cementum; ab = alveolar bone; cc = cellular cementum; de = dentine; jb = jaw bone; La = labial side; Li = lingual side; ps = periodontal space; pu = pulp cavity; vs = vascular spaces

the first and third alveoli, whereas the second and fourth alveoli are empty. The dentary (Figure 7; Figure S7) contains two fully erupted tooth crowns and two empty alveoli. The anterior and posterior edges of the bone are damaged, but the preservation is sufficient to examine tooth attachment in detail. The preserved crowns occupy the first and the fourth alveoli, the second and fifth

alveoli are empty, and a replacement tooth occupies the third alveolus.

**Histology:** The roots of the fully erupted functional teeth (Figures 5a and 7a) have a layer of globular dentine (with an average thickness of 20  $\mu\text{m}$ ) separating the orthodentine from the root cementum (e.g., Figure 8). The dental tubules of dentine extend across the entire

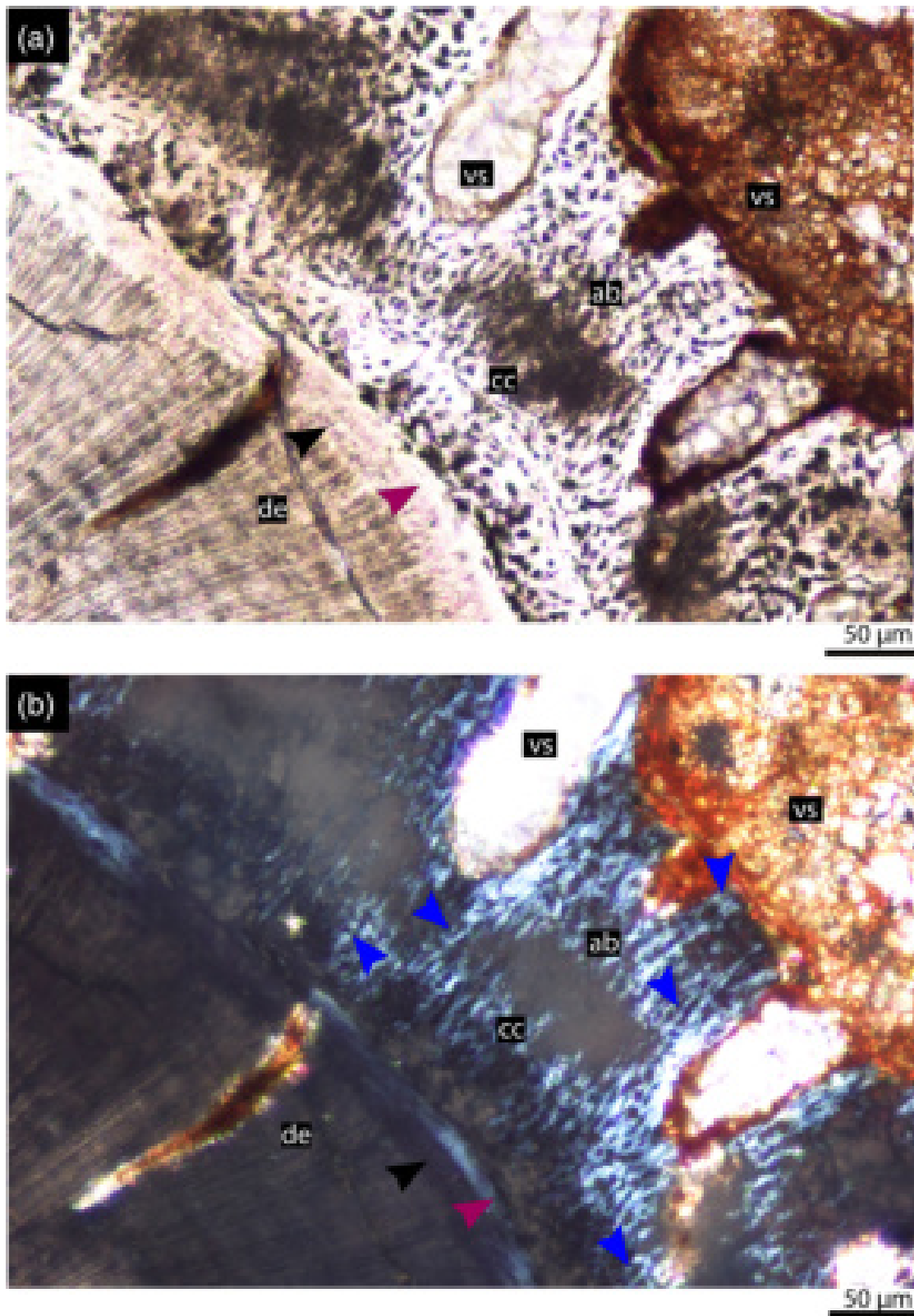


**FIGURE 8** UFSM 11579 right dentary, dental tissues in transverse section at root level. (a) Details of the tooth positioned in the first alveolus, showing the alveolar bone and cellular cementum contact (mineralized periodontal space). (b) “a” under cross-polarized light, showing Sharpey’s fibers (blue arrows) across the cellular cementum and alveolar bone layers. ab = alveolar bone; cc = cellular cementum; de = dentine; vs = vascular spaces. Black arrow indicates the layer of globular dentine; purple arrow indicates the acellular cementum

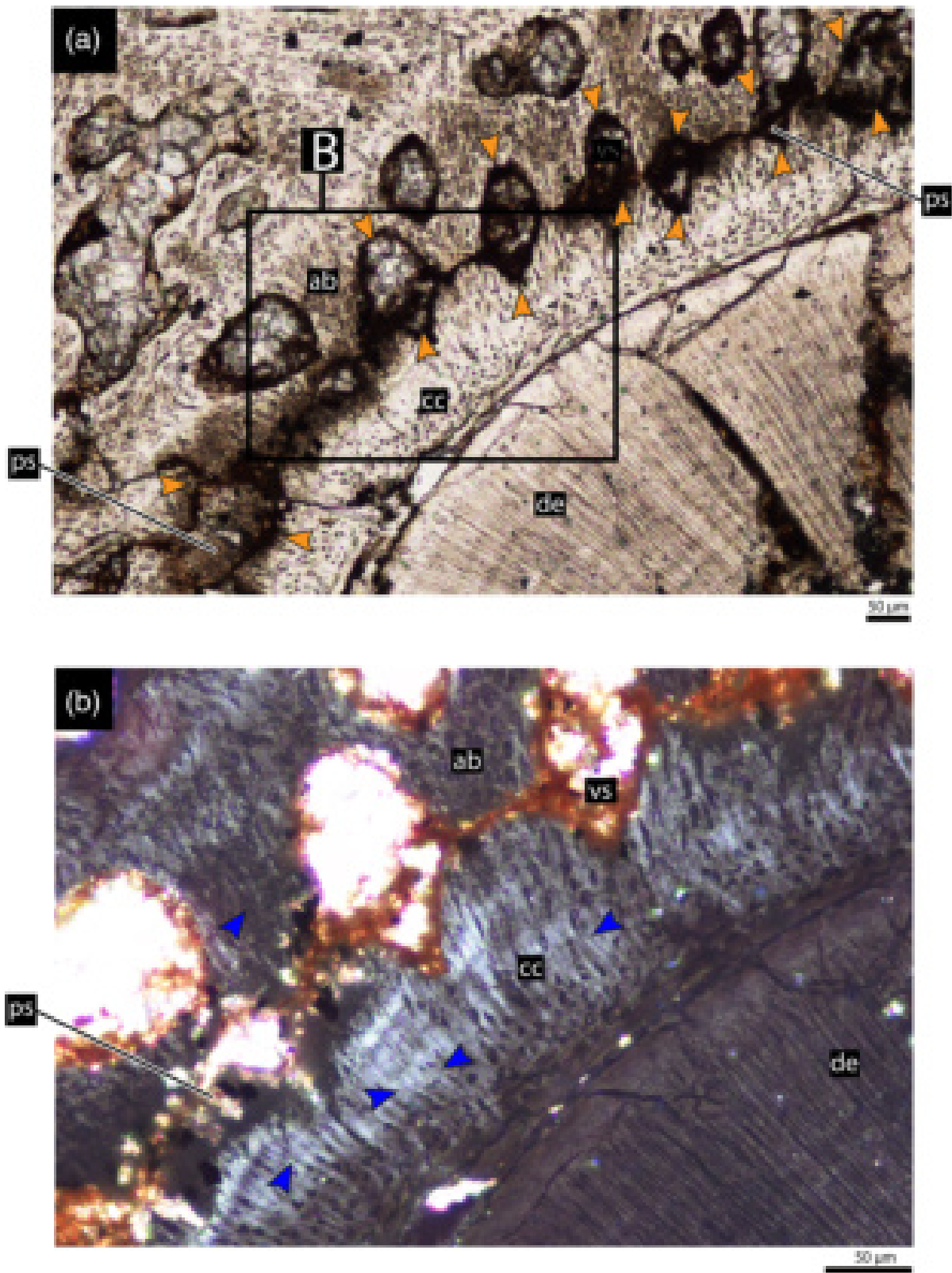


**FIGURE 9** UFSM 11579 right dentary, dental tissues in transverse section at root level. Tooth in the fourth alveolus position. (a) Tooth attachment details showing the wavy periodontal space. (b) “a” under cross polarized light, showing Sharpey’s fibers (blue arrows) across the cellular cementum and alveolar bone layers. ab = alveolar bone; cc = cellular cementum; de = dentine; ps = periodontal space; vs = vascular spaces. Orange arrow indicates vascular spaces

thickness of the teeth. The acellular cementum forms a bright and thin band (ca. 13  $\mu\text{m}$  in the maxilla and 11  $\mu\text{m}$  in the dentary; Figures 6 and 8) around the roots, whereas the cellular cementum forms a thicker layer (ca. 100  $\mu\text{m}$  in the maxilla and 91  $\mu\text{m}$  in the dentary—Figures 6a and 8a). The cellular cementum contains cementocyte lacunae arranged randomly, with a shape varying from oval to round. Under cross-polarized light, it is possible to see numerous Sharpey's fibers traversing the full thickness of the cellular cementum and radiating around the circumference of the roots toward the alveolar bone (Figures 6b, 8b and 9b). The alveolar bone in UFSM 11579 forms a thicker layer compared to that of cellular cementum (ca. 300  $\mu\text{m}$  in the maxilla and 370  $\mu\text{m}$  in the dentary) and comprises a woven bone matrix, with cells arranged in no recognizable pattern. The alveolar bone is vascularized with circular vascular channels (Figures 6 and 9) that extend dorsoventrally. The osteocyte lacunae have the same morphology and density as in the cellular cementum. The alveolar bone is a primary (unremodeled) tissue, with simple vascular canals and occasional primary osteons, as indicated by the presence of lamellar bone surrounding the channels (Figures S8–S10; LeBlanc & Reisz, 2013; LeBlanc et al., 2017; Reid, 1996). The contacts between the alveolar and the jaw bones are outlined by a distinct reversal line, marking the farthest extent of bone resorption among successive tooth replacement cycles (Fong et al., 2016). The jawbone (ca. 290  $\mu\text{m}$  in the maxilla and 125  $\mu\text{m}$  in the dentary) consists of parallel-fibered bone, in which the cells are flat, organized in an anteroposterior fashion. Its contact with the alveolar bone is clearly marked by different patterns of cell organization; the osteocyte lacunae are arranged in rows in the jawbone and with no clear pattern in the alveolar bone. The primary vascular channels extend anteroposteriorly, appearing as long and mediolaterally thin lines in cross section (Figures 5a and 7a; Figure S8B).

Two different layers of alveolar bone are present on the labial side of the third tooth of the maxilla and the fourth tooth of the dentary, with each of their boundaries outlined by a distinct reversal line (Figures S8 and S11). These lines indicate resorption and redeposition of the new layers of alveolar bone during successive tooth replacement cycles (Fong et al., 2016). The innermost layers of alveolar bone (Figures S8 and S11) correspond to the most recently deposited layer, belonging to the functional teeth.

The teeth occupying the first alveolus of the maxilla (Figure 5b,d) and the fourth alveolus of the dentary (Figure 7d,g) are in a gomphosis stage of attachment, in which there is a periodontal space between the cementum and the alveolar bone. The periodontal space varies

its thickness around the root circumference of the maxillary tooth, being thicker lingually (ca. 89  $\mu\text{m}$ ) than on the labial (ca. 36  $\mu\text{m}$ ) side, whereas the thickness is about 11  $\mu\text{m}$  around the dentary tooth. This size difference is associated with the ontogenetic stage of the teeth, in which a broader periodontal space represents an earlier stage, whereas the thinner periodontal space results from alveolar bone being deposited for a longer amount of time. The margins of the cementum and alveolar bone are wavy rather than straight, because of the presence of partially enclosed vascular channels (Figures 5d and 9; Figure S10). The tooth occupying the third alveolus of the maxilla (Figure 5c,e) and the first alveolus of the dentary (Figures 7b,e and 8) are in ankylosis stage, with the periodontal space totally closed (mineralized).

The empty alveoli of the maxilla and dentary have different outlines. The second alveolus of the maxilla is ovoid and regular (Figure 5a), possessing small layers of alveolar bone deposited at the lingual side. It seems that the tooth of the second alveolus was in the process of erupting into the mouth and then was displaced post-mortem (teeth make small layers of alveolar bone while they are in the process of erupting toward the oral cavity—see LeBlanc et al., 2018), after the ligament decayed (LeBlanc et al., 2018; LeBlanc & Reisz, 2013). It indicates that that tooth was in an earlier stage than the other teeth of this jaw. In addition, the presence of a resorption pit lingual to this alveolus and the presence of two chunks of dentine from an old tooth at the labial side is further evidence that a replacement tooth was erupting into the jaw, taking over the post-mortem displaced tooth position (LeBlanc & Reisz, 2013). The fourth alveolus of the maxilla (Figure 5a; Figure S9B) and the second of the dentary (Figure 7a; Figures S12B1 and S13) are rounded and regular, which seem to preserve socket walls with well-developed alveolar bone. These teeth were likely held in place by an unmineralized ligament and fell out of the sockets post-mortem (the same situation of the tooth in the second alveolus of the maxilla), as observed in taxa with a gomphosis-type of tooth attachment, such as dinosaurs, crocodylians, and mammals (LeBlanc & Reisz, 2013; LeBlanc et al., 2017; LeBlanc et al., 2018).

As mentioned above, remnants of dentine from previous tooth generations are embedded within the labial walls of the alveoli in the maxilla (Figure 5a; Figure S9). These dentine remnants are heavily resorbed, and the most complete fragment is embedded within the alveolar bone anterior to the first alveolus. This remnant nearly preserves the complete circumference of an old root, indicating that the tooth was much smaller (approximately  $\frac{1}{4}$  the size) than the current generation of functional teeth. Its small size suggests that it corresponds to a much earlier generation of tooth from when this animal was

younger. The positions of the dentine fragments relative to the functional teeth indicate that the functional teeth have migrated lingually relative to previous tooth generations (Figure 5a; Figure S9). The dentary also bears one small tooth remnant positioned between the fourth and fifth alveoli (Figure 7a; Figure S11A).

The erupting replacement tooth of the dentary has a “kidney” shape in a cross-section. In a more apical cross-section, it is possible to see the enamel cap of the replacement tooth (Figure S12A), which gives way to the attachment tissues of the developing root in deeper sections (Figure S12B). These sections reveal a thin layer of acellular cementum (ca. 6  $\mu\text{m}$ ), followed by a thicker layer of cellular cementum (ca. 36  $\mu\text{m}$ ) in replacement teeth, showing that those tissues were present even in an early stage of tooth development. Surrounding the replacement tooth there is a partially resorbed piece of the replaced tooth. This piece was not part of a functional tooth, but its attachment tissues are still evident. In this case, the old tooth was ankylosed to the jaw, with the periodontal space totally mineralized by the alveolar bone (Figure 7c,f), as expected for the fixation of a tooth in a later ontogenetic stage.

### 3.3 | *Sacisaurus agudoensis*

One incomplete right dentary of *S. agudoensis* (MCN PV 10095) was sectioned (Figure S14), containing one fully erupted tooth crown and eight empty alveoli (Figures 10 and 11). The anterior and posterior edges of the bone are missing, but the tooth and its attachment tissues are well preserved. The preserved tooth occupies the fifth alveolus (Figure 10a).

**Histology:** The only preserved tooth consists of a dentine core, which is entirely traversed by dental tubules. The dentine is coated in a thin (ca. 9  $\mu\text{m}$ ) layer of acellular cementum. Under cross-polarized light, it appears as a bright band outlining the root (Figure 11). The cellular cementum (Figure 11) is more than five times thicker than the acellular layer (ca. 57  $\mu\text{m}$ ). It contains many oval or circular randomly-distributed cementocyte lacunae. Cross-polarized light shows a network of Sharpey's fibers across the entire thickness of the cellular cementum and alveolar bone layers (Figure 11). The cementum and the alveolar bone contact one another, with the complete mineralization of the periodontal space indicating the tooth is at the ankylosis stage (Figures 10c and 11). The resorption pit present in the lingual side of the jaw (Figure S14A) confirms that the tooth is at a late ontogenetic stage, even though there is no trace of the replacement tooth in the histologic sections.

The alveolar bone is formed by a woven bone matrix, with numerous simple vascular channels. These vascular channels are simple circular canals in cross section, indicating that the vasculature extended dorsoventrally (Figure 11) within the alveolar bone, near its contact with the cellular cementum. The alveolar bone layer is thicker (ca. 145  $\mu\text{m}$ ) than the cellular cementum layer (ca. 57  $\mu\text{m}$ ). As is typical of the woven-fibered matrix of alveolar bone (Fong et al., 2016), the osteocyte lacunae are randomly distributed. The boundary between the alveolar and the jawbone is outlined by a reversal line, which is very distinct under cross-polarized light (Figure 11). The jaw bone is approximately 142  $\mu\text{m}$  thick and formed by parallel-fibered bone. The cells are longer anteroposteriorly than lateromedially (Figure 11) and arranged in anteroposteriorly-directed rows (Figure 10a). Under cross-polarized light, the jaw bone is brighter than both the alveolar bone and cellular cementum. The primary vascular channels are longer anteroposteriorly and some of them branch (Figure 11). Poor preservation of the margins of the empty alveoli makes it difficult to determine if they form regular or irregular outlines, which would indicate whether the teeth were held in place by gomphosis or ankylosis (LeBlanc & Reisz, 2013; LeBlanc et al., 2017; LeBlanc et al., 2018).

### 3.4 | *Asilisaurus kongwe*

Two specimens of *A. kongwe* (NMT RB 1086; NMT RB 1087; Figures S15 and S16; Figures 12–14) have been sampled, both of which preserve several in-situ teeth. NMT RB 1086 is a partial right dentary, preserving its anterior tip (i.e., prementary equivalent of Ferigolo & Langer, 2007; Langer & Ferigolo, 2013), and the seven anterior-most teeth (Figure 12a). NMT RB 1087 preserves 11 empty alveoli and eight tooth crowns. Because of its poor preservation, we could not differentiate the lingual from the labial surfaces of NMT RB 1087 and consequently its anatomical position along the jaw. The preserved teeth occupy alveoli 1, 2, 3, 5, 6, 7, 8, and 11 (Figure 13a). Due to damage, the contour of the roots is incomplete in some teeth (e.g., teeth 1, 3, and 4 in NMT RB 1086, and teeth 2, 3, and 6 in NMT RB 1087).

**Histology:** The tooth roots are circular in cross-section and are entirely cored by dentine, with the dental tubules extending across their entire thickness. The roots are coated in a thick layer (ca. 18  $\mu\text{m}$ ) of globular dentine separating the orthodentine from the root cementum (Figure 14). This corresponds to the granular layer of Tomes (Nanci, 2013), as also observed in the neotheropod dinosaur *Coelophysis bauri* (Fong et al., 2016). The globular dentine has a yellow aspect (Figures 14a,b) that

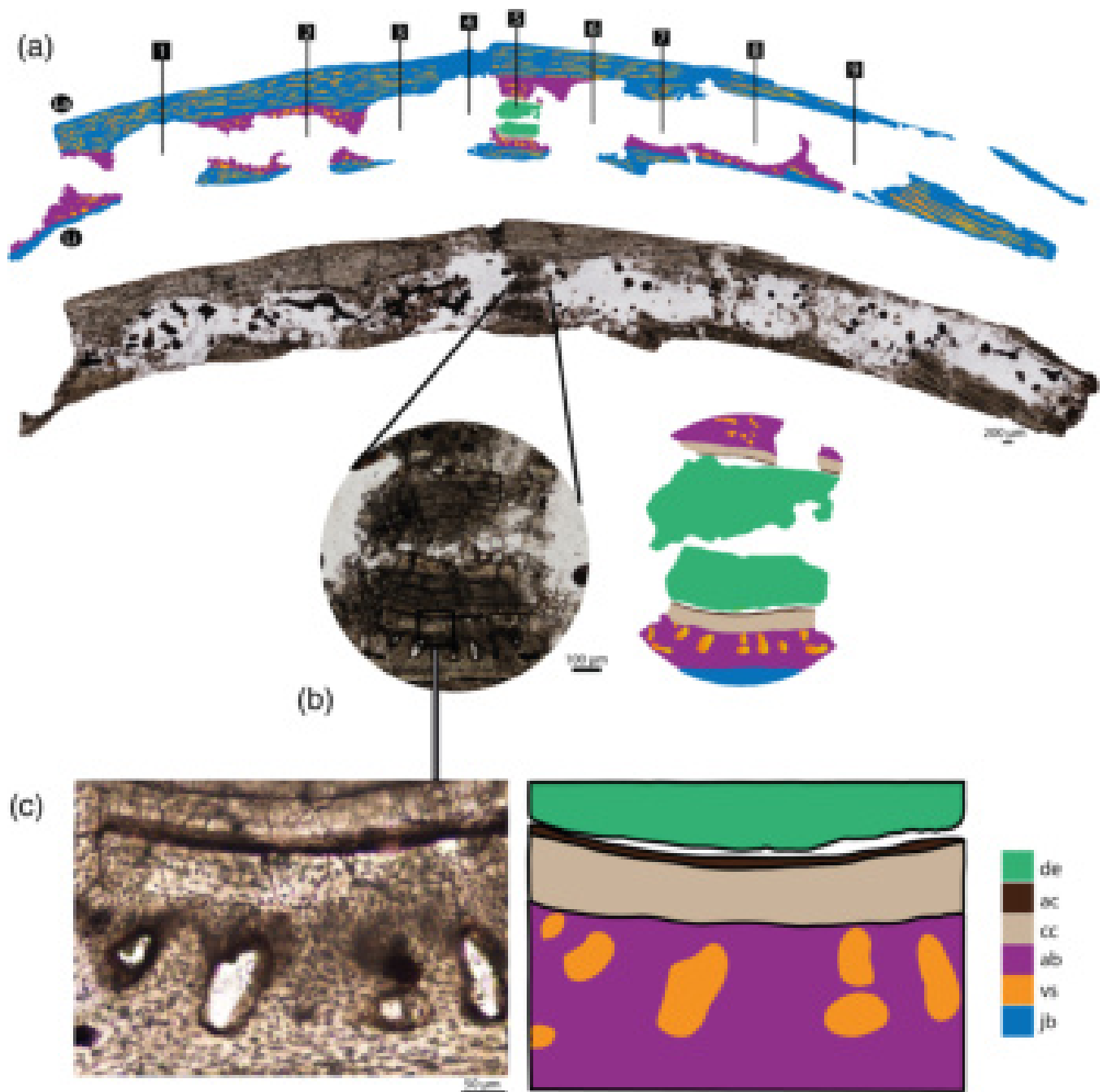


**FIGURE 10** *Sacisaurus agudoensis* (MCN-PV 10095) right dentary, dental tissues in transverse section at root level, with diagrammatic illustrations. (a) General view. (b) Tooth of the fifth alveolus. (c) Detail of “b,” showing the contact between alveolar bone and cellular cementum. ac = acellular cementum; ab = alveolar bone; cc = cellular cementum; de = dentine; jb = jaw bone; La = labial side; Li = lingual side; vs = vascular spaces

appears dark under cross-polarized light (Figure 14c). The acellular cementum layer is thinner (ca. 10  $\mu\text{m}$ ), positioned external to the globular dentine, and differentiated from it by its brighter color (Figure 14b), even under cross-polarized light (Figure 14c). The cellular cementum is much thicker than the acellular cementum (ca. 57  $\mu\text{m}$  in NMT RB 1086 and ca. 91  $\mu\text{m}$  in NMT RB 1087). The cells are small and there is no recognizable

distribution pattern. Under cross-polarized light, numerous Sharpey's fibers traverse the cellular cementum and alveolar bone zone around the whole circumference of the root (Figure 14c). The contact between the cellular cementum and the alveolar bone are seen in all teeth, even if only in some portions (e.g., Figure 12b, Figure S17). In NMT RB 1086 (Figure 12a), parts of the periodontal space of the tooth roots are clearly mineralized, but in other

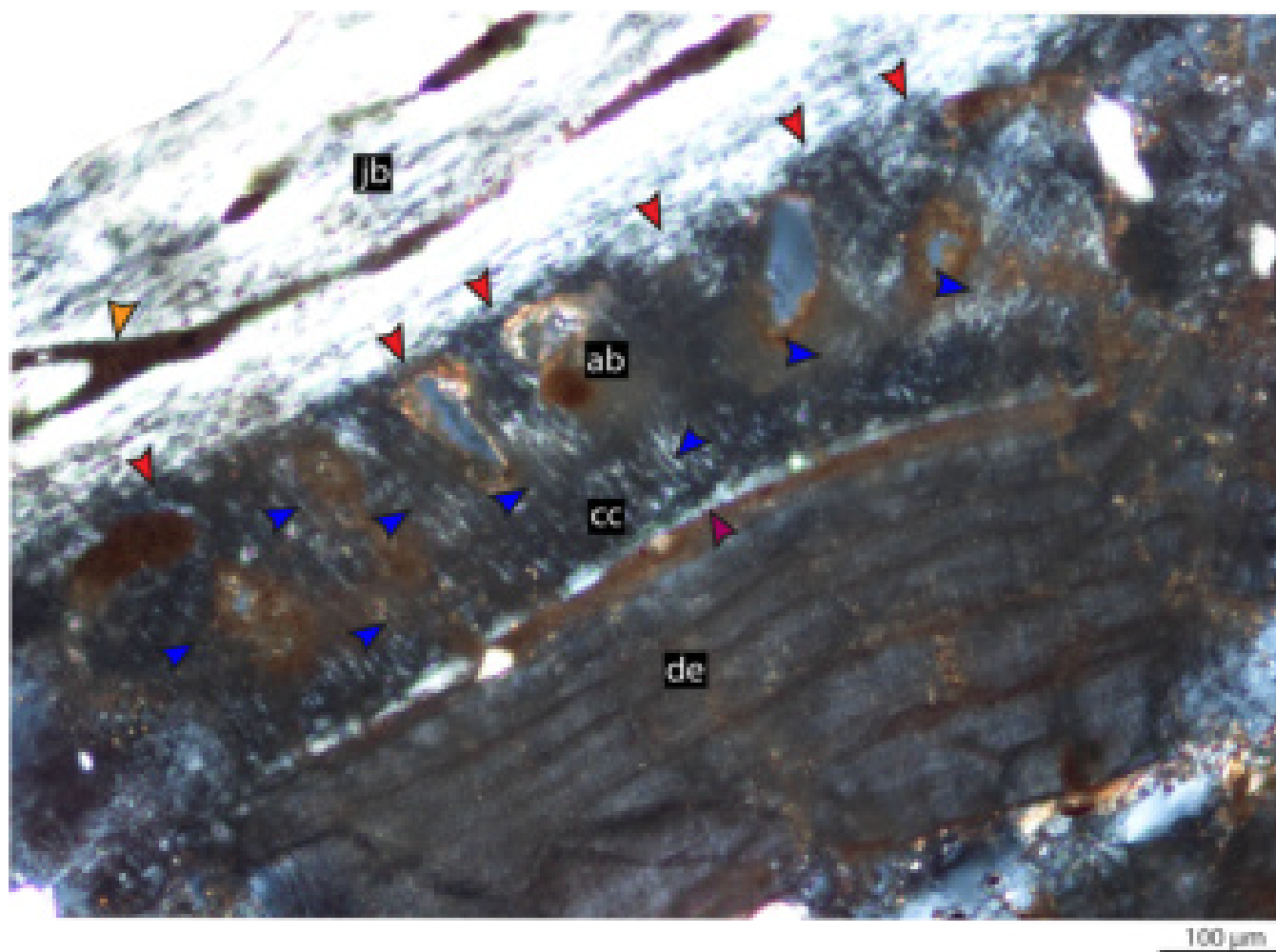


**FIGURE 11** *Sacisaurus agudoensis* (MCN-PV 10095) right dentary, dental tissues in transverse section at root level. (a) Tooth of the fifth alveolus under polarized light, showing reversal lines (red arrows) separating the alveolar bone from the jaw bone, and the presence of Sharpey's fibers (blue arrows) across the cellular cementum and alveolar bone. ab = alveolar bone; cc = cellular cementum; de = dentine; jb = jaw bone. Orange arrow = vascular space; purple arrow indicates the acellular cementum

parts it is not clear if they are not mineralized, or are taphonomically damaged. The fifth tooth of NMT RB 1086 is the only one that clearly shows parts where the cellular cementum and alveolar bone are contacting one another (evidencing ankylosis) and points where the periodontal space is still open, characterizing an intermediate “mineralization” stage (Figures 12b and 14).

The alveolar bone layer is formed by woven tissue matrix and is thicker (ca. 227  $\mu\text{m}$  in NMT RB 1086 and ca. 182  $\mu\text{m}$  in NMT RB 1087) than the cellular cementum layer. It is vascularized, with simple vascular channels that are either oval or circular in cross section. All the vascular channels are located external to the contact with the cellular cementum. The anterior margin of the seventh alveolus of NMT RB 1086 displays dentine remnants from the older tooth generation (Figure S18).

The jawbone is approximately 227  $\mu\text{m}$  thick in NMT RB 1086, and 409  $\mu\text{m}$  thick in NMT RB 1087. It is formed

by parallel-fibered (lamellar) bone, the matrix of which has an organized pattern of cell distribution. The boundary between the alveolar and jawbone is outlined by a clear reversal line (Figure S18), corresponding to the oldest deposited portion of the alveolar bone (Fong et al., 2016; LeBlanc et al., 2017; LeBlanc et al., 2018). The primary vascular channels of the jawbone are anteroposteriorly longer in cross section (Figures 12a and 13a).

## 4 | DISCUSSION

### 4.1 | Tooth attachment in silesaurids involves cementum, periodontal ligament, and alveolar bone

Historically, fused (ankylosis) teeth and those suspended by a periodontal ligament (gomphosis) were considered

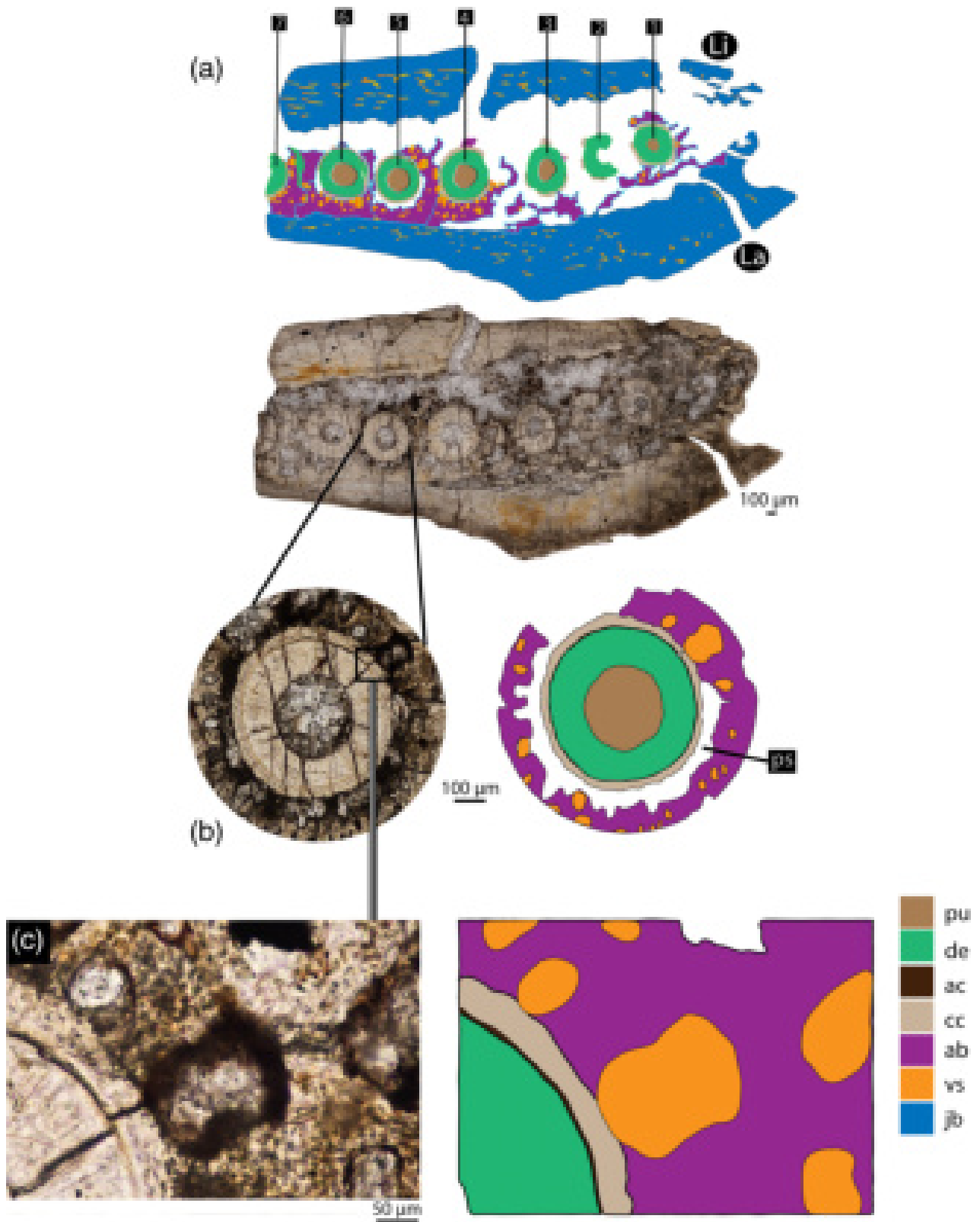


**FIGURE 12** *Asilisaurus kongwe* (NMT RB 1086) right dentary, dental tissues in transverse section at root level, with diagrammatic illustrations. (a) General view. (b) Tooth of the fifth alveolus, showing the mineralization stage. (c) Detail of “b,” showing the contact between alveolar bone and cellular cementum. ac = acellular cementum; ab = alveolar bone; cc = cellular cementum; de = dentine; jb = jaw bone; La = labial side; Li = lingual side; ps = periodontal space; pu = pulp cavity; vs = vascular spaces

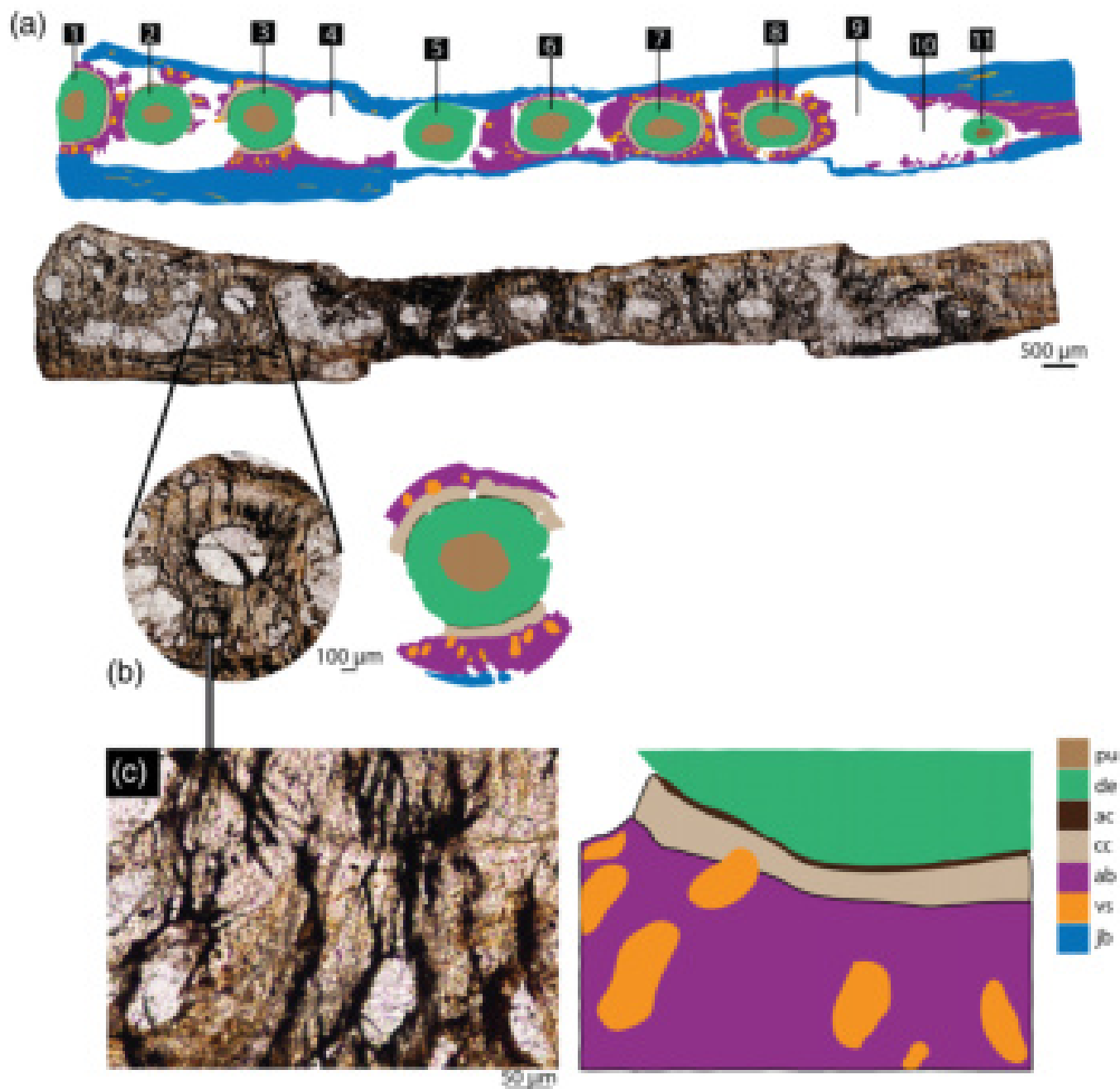


**FIGURE 13** *Asilisaurus kongwe* (NMT RB 1087) dentary, dental tissues in transverse section at root level, with diagrammatic illustrations. (a) General view. (b) Tooth of the third alveolus. (c) Detail of “b,” showing the contact between alveolar bone and cellular cementum. ac = acellular cementum; ab = alveolar bone; cc = cellular cementum; de = dentine; jb = jaw bone; La = labial side; Li = lingual side; pu = pulp cavity; vs = vascular spaces

plesiomorphic and derived tooth attachment systems in amniotes, respectively, involving different periodontal tissues (Osborn, 1984; Peyer, 1968; Tomes, 1874; Zaher & Rieppel, 1999). Silesaurid tooth attachment has been interpreted as a case of ankylosis (Langer & Ferigolo, 2013; Martz & Small, 2019; Nesbitt, 2011; Nesbitt et al., 2010, 2020), which differs from the gomphosis of all dinosaurs and Crocodyliformes

documented to date (Kvam, 1960; LeBlanc et al., 2017; McIntosh et al., 2002; Miller, 1968). Yet, our histological study revealed a more complex situation, with each sample revealing a combination of tooth attachment modes. We identified both gomphosis and ankylosis in fully erupted teeth of silesaurids, as well as an intermediate mineralization phase (*sensu* LeBlanc et al., 2018), where the periodontal space is only partially invaded by the

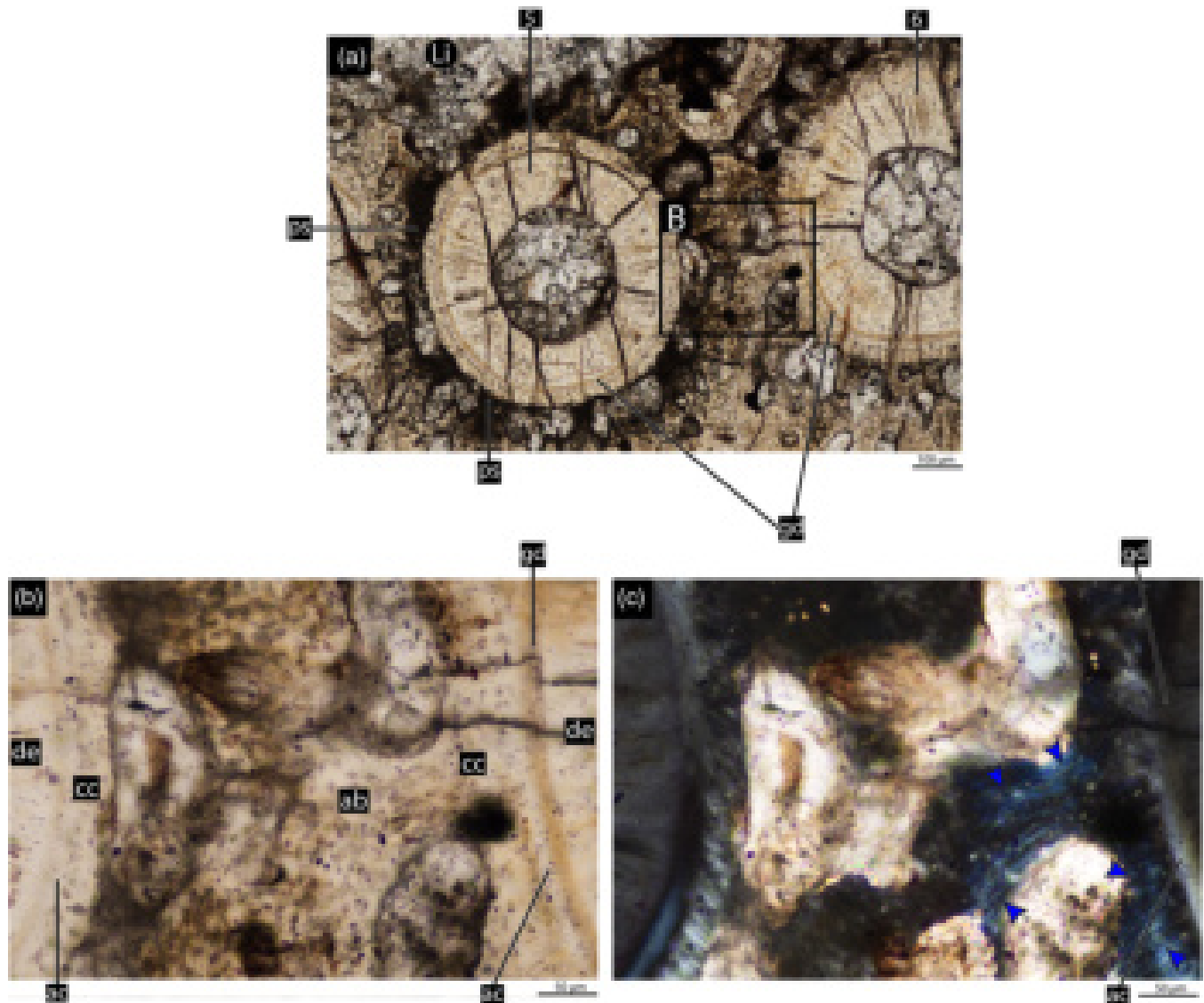


**FIGURE 14** *Asilisaurus kongwe* (NMT RB 1086) dentary, dental tissues in transverse section at root level. (a) Teeth of the fifth and sixth alveoli, showing the mineralization stage. (b) Tooth attachment details of an area in “a,” showing the contact between alveolar bone and cellular cementum. (c) “b” under cross-polarized light, showing Sharpey’s fibers (blue arrows) across the cellular cementum and alveolar bone layers. ac = acellular cementum; ab = alveolar bone; cc = cellular cementum; de = dentine; gd = globular dentine; Li = lingual side; ps = periodontal space

encroaching alveolar bone (Figures 1, 5, 6, 9, 10 and 12). In addition, the presence of Sharpey’s fibers, root cementum, and discrete layers of alveolar bone indicates that silesaurids display all three tooth attachment tissues that have traditionally been restricted to mammalian and crocodylian teeth (Figures 3, 6, 8, 9, 11 and 14) (Peyer, 1968; Tomes, 1874). Their presence in silesaurids, as well as their recent discoveries in numerous other amniote groups, indicates that root cementum, alveolar bone, and periodontal ligament are actually symplesiomorphic for Amniota, echoing previous studies (Caldwell et al., 2003; LeBlanc et al., 2017; LeBlanc et al., 2018; Maxwell et al., 2011; Pretto et al., 2014).

In amniotes with a gomphosis-type of tooth fixation, the periodontal space persists throughout tooth development (Fong et al., 2016; LeBlanc et al., 2017; LeBlanc et al., 2018). Among the studied silesaurids, this condition was identified in both the Hayden Quarry (Figure 1a,b,d,e) and Santa Maria Formation (Figures 5b, d, 7d,g and 9) silesaurids, whereas most teeth of *A. kongwe* were in the mineralization stage (Figure 12a, b). In all these forms, the periodontal space that once housed the periodontal ligament persists between tooth root and surrounding alveolar bone. Alveolar bone is the thickest and the most abundant mineralized attachment tissue in all of the silesaurid specimens analyzed here.

This highly vascularized bone grew centripetally (towards the cementum coating the tooth roots), gradually reducing the periodontal space to a thin and uneven sliver in teeth at the intermediate mineralization stage (Figures 12a,b and 14a).

Ankylosed teeth are present in all of the specimens (e.g., GR 1072 [Figure 1c,f], UFSM 11579 [Figures 6 and 8]). Ankylosis in Silesauridae occurs via the continued growth of alveolar bone towards the cellular cementum coating each tooth root, causing the complete closure of the periodontal space and the mineralization of the periodontal ligament within the alveolar bone and cementum (e.g., see Figure 8 compared to Figure 9). This mineralization pattern differs from that of some other reptiles with an ankylosis type of fixation, such as the extinct marine mosasauroid squamates, or the shell-crushing teiid squamate *Dracaena*, in which the cellular cementum is the thickest tissue and grows toward the alveolar bone layer (Caldwell et al., 2003; LeBlanc et al., 2020). The process of ankylosis in silesaurids mirrors that of many early synapsids (LeBlanc et al., 2016, 2018), where the teeth are initially held in place by gomphosis, followed by the gradual growth of the alveolar bone towards the tooth root, eventually fusing the tooth in its socket.

## 4.2 | Evidence for delayed ankylosis in silesaurids

Despite the observation that teeth fuse to the jaws in the latest stages of dental ontogeny in silesaurids, several teeth in our sample shows evidence of gomphosis (Table 2). This suggests that silesaurid teeth spent considerable time attached to the jaws via a non-mineralized periodontal ligament prior to fusing in place. Several histological details support this conclusion. First, we identified growth lines in the cellular cementum of the Hayden Quarry silesaurid (Figure 2). Growth lines in the cementum of ankylosed teeth (e.g., tooth in alveolus 3; Figure 2a) reveals a relatively prolonged gomphosis phase, because they can only be produced when there is periodontal space around a tooth, leaving enough space for cementum layers to accumulate outwards (LeBlanc et al., 2018; LeBlanc & Reisz, 2013). Sharpey's fibers also penetrate into the deepest layers within the cementum (Figure 3b). These correspond to the attachment points of the periodontal ligament, which clearly suspended the tooth within its alveolus for a considerable time while the cementum was accumulating along the root surface (Caldwell et al., 2003; LeBlanc et al., 2017; LeBlanc et al., 2018; LeBlanc & Reisz, 2013).

Second, we observed several instances of extensive tooth drift—a process through which teeth move along

the jaws via remodeling of the periodontal ligament and alveolar bone—within the jaws of these silesaurids. This is a very common phenomenon in mammals (Saffar, Lasfargues, & Cherruau, 1997) and dinosaurs (Bramble, LeBlanc, Lamoureux, Wosik, & Currie, 2017; Chen et al., 2018; He, Makovicky, Xu, & You, 2018), where the periodontal ligament remains permanently non-mineralized. The same phenomenon occurs in several Permian therapsids (early synapsids), where the periodontal ligament remained non-mineralized long enough to allow for tooth drift (LeBlanc et al., 2018) before eventually fusing each tooth in place. In extinct forms, large fragments of old tooth generations preserved within the jaws provide evidence for tooth drift, because these unresorbed remains of older teeth were far enough away to avoid being completely resorbed during subsequent tooth replacement events (He et al., 2018; LeBlanc et al., 2018). We observed large dentine fragments within the bone tissues of the dentary and maxilla of UFSM 11579 at nearly every tooth position and in between some teeth of *A. kongwe* (Figures 5a, 7a and 15b; Figures S9, S11A and S18). This suggests that mesio-distal and lingual tooth drift occurred in these jaw elements, which had to be mediated by a fairly prolonged ligamentous phase of tooth attachment.

Summarizing the above information and considering empty alveoli as evidence of gomphosis (LeBlanc et al., 2018; LeBlanc & Reisz, 2013), the specimens studied here can be interpreted as follows (Table 3): GR 1072 (Hayden Quarry silesaurid)—alveolus 3 ankylosed, alveoli 1, 2, 4, 6, 7 and 8 with gomphosis; UFSM 11579 (Santa Maria Formation silesaurid)—maxillary alveolus 3 and dentary alveolus 1 ankylosed; maxillary alveoli 1, 2 and 4 and dentary alveoli 2 and 4 with gomphosis. Such a detailed account is not feasible for *S. agudoensis* and *A. kongwe*, but it is clear that both gomphosis and ankylosis were present. In addition, the “intermediate” stage, characterized by an incomplete ankylosis of a tooth root to the socket (LeBlanc et al., 2018), was found in both *A. kongwe* (Figure 14a) and the Hayden Quarry silesaurid (Figures S4C and S5C). In the latter form, the two most apical sections of the tooth in alveolus 1 are in the gomphosis stage (Figure S5A,B), whereas its most basal section is in the mineralization stage (Figure S5C). In the same way, the two most apical sections of the tooth in alveolus 3 indicate an ankylosis stage (Figure S4A, B), whereas its most basal section is in the mineralization stage (Figure S4C). This means that the process of mineralization progressed at different rates throughout the tooth length.

Different stages of tooth development are present in our silesaurid samples; from erupting replacement teeth, teeth under resorption, to remains of old tooth generations. In alveolus 5 of the Hayden Quarry silesaurid

**TABLE 2** The total number of teeth at the eruption, gomphosis, mineralization and ankylosis stages (not considering empty alveoli here) in thin sections, reflecting the proportion of time teeth spend in the respective stages

Specimen	Total number of teeth	Total number of teeth in each stage/Alveoli position			
		Eruption	Gomphosis	Mineralization	Ankylosis
Hayden Quarry silesaurid (GR 1072)	4	1/5°	2/1°, 8°	2/1°, 3°	1/3°
UFSM 11579—maxilla	2	0	1/1°	0	1/3°
UFSM 11579—dentary	3	1/3°	1/4°	0	1/1°
<i>Sacisaurus agudoensis</i>	1	0	0	0	1/5°
<i>Asilisaurus kongwe</i> 1086	7	0	?	1/5°	?
<i>Asilisaurus kongwe</i> 1087	8	0	?	?	?

*Note:* Note that the number of teeth do not match the exactly number of teeth in each phase because there can be more than one thin section for the same tooth (see Figures S4 and S5).

(Figure 4) and in alveolus 3 of the Santa Maria Formation silesaurid lower jaw (Figure 7c), the old tooth pieces provide information about tooth fixation at later ontogenetic stages, terminating in ankylosis in all cases (Figures 4b, 7f and 15b,c). The replacement tooth in both forms is already in the functional position, with an enamel layer surrounding the dentine (Figure 4a; Figure S12A2). However, a more basal cross-section of the UFSM 11579 younger tooth already shows attachment tissues, (acellular and cellular cementum [Figure S12B3]). A similar arrangement of old tooth pieces is present in the neotheropod dinosaur *C. bauri* (Figure 15a). However, unlike in the Hayden Quarry and Santa Maria Formation silesaurids, the old tooth generation of *C. bauri* still have unmineralized periodontal space, with no contact between the cementum and the alveolar bone, (i.e., gomphosis) enduring until the last stage of tooth development (Figure 15). *Asilisaurus kongwe* also has an old tooth generation near a functional tooth, but only its dentine is preserved, with all attachment tissues already resorbed (Figure 12a; Figure S18). This is also the case for both maxilla and dentary of UFSM 11579, in which such teeth are smaller than the functional teeth in dorsal view (“lt” in Figures S9A-C and S11A).

### 4.3 | Reconstructing tooth attachment ontogeny in Silesauridae: Implications for phylogenetic analyses

The simple mapping of “ankylosis” and “gomphosis” as alternative character states is too simplistic to reconstruct ancestral tooth attachment across archosaur phylogenies (similar to the Synapsida, LeBlanc et al., 2018). In part, this is because silesaurids have here been shown to have both states in the same taxon, individual, and jaw quadrant, and this may also apply to other unsampled

members of the group. Instead, we identified four different phases of a standard sequence of dental ontogeny in the sampled silesaurids: eruption, gomphosis, mineralization, and ankylosis (Table 2; Figure 16). This sequence was also described for synapsids (LeBlanc et al., 2018), where each tooth in a thin section of a jaw can be staged based on the relative development of the periodontal tissues.

The earliest stage is tooth eruption, when the tooth is actively replacing an old tooth, but is not yet functional (Figure 16a). In our silesaurid sample, replacement events have been documented only in the Hayden Quarry and Santa Maria Formation silesaurids. Very thin layers of alveolar bone are present both labial and lingual to the developing tooth, representing the initial stage of the socket development in the tooth. The replacement tooth in the third alveolus of the dentary of UFSM 11579 has dentine and thin layers of acellular and cellular cementum in a more basal cross-section (Figure S12). The condition in these silesaurids differs from that of mammals, crocodylians, and dinosaurs, in which the cellular cementum is only deposited when the tooth is already functional (LeBlanc et al., 2017). The newly-formed teeth develop within resorption pits along the lingual side of the dentary, as is typical for amniotes (Edmund, 1960; Richman & Handrigan, 2011; Zaher & Rieppel, 1999), including some dinosaurs (Fong et al., 2016). Such pits can be seen in the lingual side of the *S. agudoensis* jaw (Figure S14), as well as in various other silesaurids (Langer & Ferigolo, 2013; Martz & Small, 2019; Nesbitt et al., 2020), theropods (Fong et al., 2016; LeBlanc et al., 2017) and ornithischians (Chen et al., 2018; LeBlanc et al., 2017). The location of the developing replacement teeth in Silesauridae suggests that the position of the odontogenetic organ (dental lamina) is the same as in most amniotes, including dinosaurs: closer to the gum line (Edmund, 1960; Fong

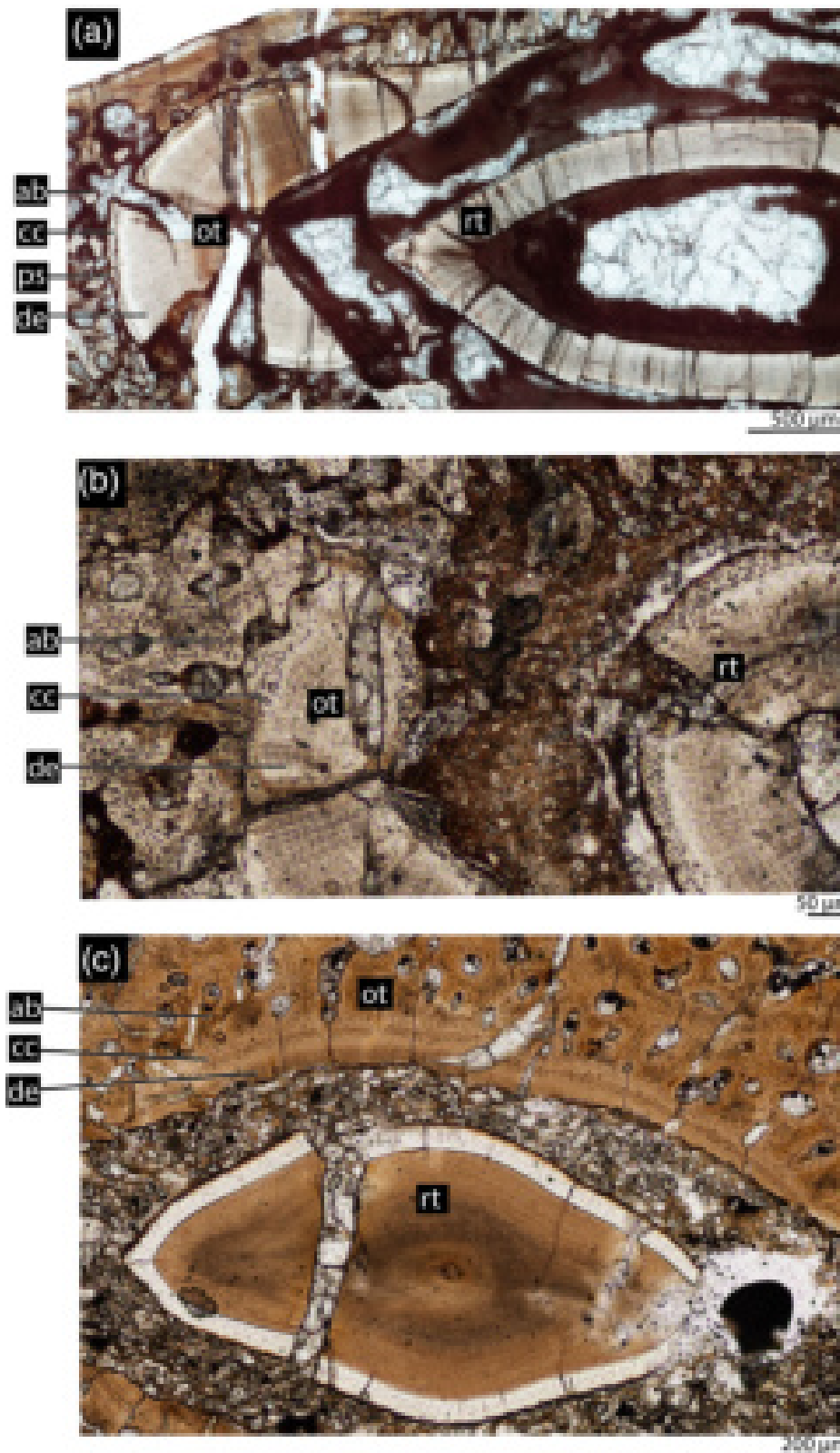


**FIGURE 15** Dental tissues of the dentary of three different taxa with teeth at the same odontogenetic stage; that is, replacement tooth being surrounded by a piece of the replaced tooth (old tooth generation).

(a) *Coelophysis bauri* (from LeBlanc et al., 2017). (b) UFSM 11579 (Figure 7c,f). (c) Hayden Quarry silesaurid (Figure 4). ab = alveolar bone; cc = cellular cementum; de = dentine; ps = periodontal space; ot = old tooth generation; rt = replacement tooth

et al., 2016; Wu et al., 2013), rather than buried deep within the jaw as in crocodylians (Fong et al., 2016; LeBlanc et al., 2017; Martin & Stewart, 1999).

The second stage is gomphosis, where the tooth is fully erupted, functional, and suspended in place by a

periodontal ligament attached to the root cementum and alveolar bone (Figure 16b). This stage is present in several tooth positions in our silesaurid sample (Table 2; Figures 1, 5, 7 and 9). The periodontal space around each tooth root in this stage is complete; it surrounds the

**TABLE 3** The total number of teeth at the eruption, gomphosis, mineralization and ankylosis stages (considering empty alveoli here) in thin sections, reflecting the proportion of time teeth spend in the respective stages

Specimen	Total number of teeth	Total number of empty alveoli	Total number of teeth in each stage/Alveoli position			
			Eruption	Gomphosis	Mineralization	Ankylosis
Hayden Quarry silesaurid (GR 1072)	4	4	1/5°	6/1°, 2°, 4°, 6°, 7°, 8°	2/1°, 3°	1/3°
UFSM 11579—maxilla	2	2	0	3/1°, 2°, 4°	0	1/3°
UFSM 11579—dentary	3	1	1/3°	2/2°, 4°	0	1/1°
<i>Sacisaurus agudoensis</i>	1	8	0	?	?	1/5°
<i>Asilisaurus konwge</i> 1086	7	0	0	?	1/5°	?
<i>Asilisaurus kongwe</i> 1087	8	3	0	?	?	?

Note: Note that the number of teeth do not match the exactly number of teeth in each phase because there can be more than one thin section for the same tooth (see Figures S4 and S5).

entire tooth, indicating that the alveolar bone has not reached the root cementum. This is a transient stage in silesaurids, but a permanent condition in mammals, crocodylians, dinosaurs, and several other amniotes (LeBlanc et al., 2017, 2018; Maxwell et al., 2011; McIntosh et al., 2002).

The third stage is termed the mineralization stage and is more difficult to identify (Figure 16c). Teeth in this stage are partially ankylosed, where the periodontal space is closed in some, but not all regions around the tooth (e.g., Figures 12b and 14; Figures S4C and S5C). This intermediate stage is presumably short-lived in most taxa, given how rare it is in our histological sample (Table 2), as well as in those of other amniotes (LeBlanc et al., 2018). The final stage is complete ankylosis (Figure 16d), where the periodontal space is completely closed, the cementum and alveolar bone contact all around the tooth root, and the periodontal ligament has become completely mineralized (e.g., Figures 1c, 3, 5c, e and 11). The full replacement cycle is completed when the replacement tooth and pit causing the resorption of the surrounding dentine and periodontal tissues (e.g., Figure S14) enlarge and invade the pulp cavity of the functional tooth. Then, the functional tooth is shed and the replacement tooth, which is already attached via periodontal ligaments, begins to migrate into the oral cavity (see fig. 10 of LeBlanc & Reisz, 2013).

According to the staging scheme conceived by LeBlanc et al. (2018), there are three possible character states to be scored: (0) rapid ankylosis; (1) delayed ankylosis; and (2) permanent gomphosis. These three states depend on the relative proportions of teeth recorded in each of the four ontogenetic stages mentioned above. Silesauridae exhibit neither the crocodylian/dinosaur state (permanent gomphosis) in which ankylosis never occurs, nor the state observed in many lepidosaurs or

early amniotes (rapid ankylosis) where the gomphosis and mineralization stages are almost never observed. Instead, all sampled silesaurids exhibit state 1 (delayed ankylosis), in which teeth are frequently found in all the four stages, with the final stage being ankylosis (Figure 16). The relative proportions of teeth recorded in each stage likely indicate the relative amount of time a tooth spends in each ontogenetic stage (Tables 2 and 3).

We recommend that future phylogenetic analyses evaluate archosauriform tooth attachment based on the relative duration of the gomphosis and ankylosis phases, instead of simplifying it into the presence or absence of gomphosis. Ankylosis and gomphosis are two ends of the same ontogenetic trajectory for most amniotes, including silesaurids, and it is the timing of these events that is likely to be phylogenetically informative.

#### 4.4 | Silesauridae and the origins of dinosaur and crocodylian tooth attachment

The results presented here show that the differences between silesaurid tooth attachment and dinosaur/crocodylian gomphosis is not associated with an increase in tooth tissue complexity, but rather to differences in the timing of a common sequence of dental ontogeny (Figures 15 and 16) (LeBlanc et al., 2017). By histologically evaluating tooth attachment in silesaurids, we identified a striking instance of convergent evolution between archosaurs and synapsids. LeBlanc et al. (2018) showed that the explanation for the differences in tooth attachment across Synapsida is a heterochronic delay in the onset of ankylosis or due to progenesis/truncation of that stage of dental ontogeny, resulting in the stereotypic mammalian permanent gomphosis (LeBlanc et al., 2018). Instead of being histologically more complex, mammals

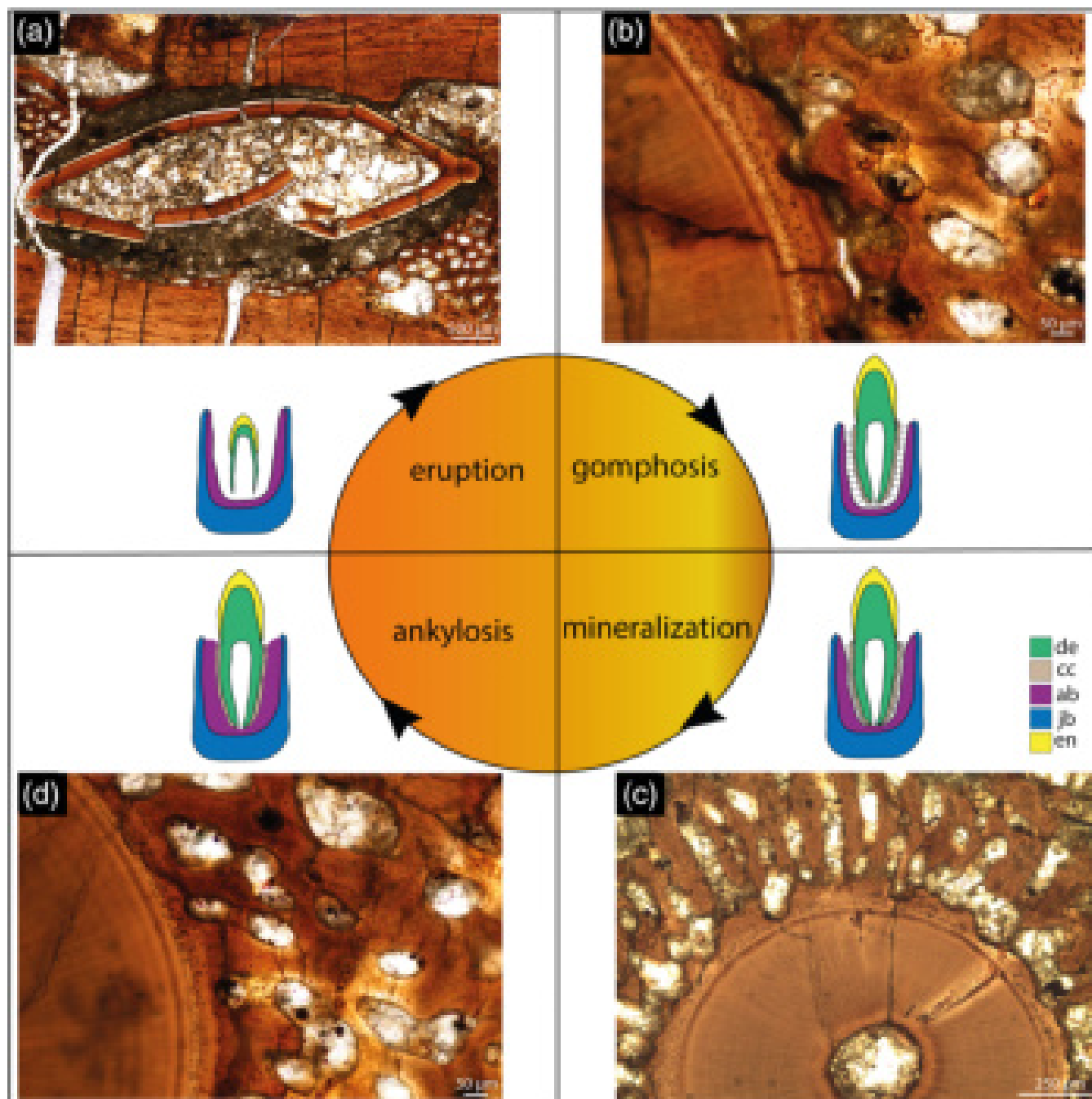


**FIGURE 16** Dental ontogeny in Silesauridae: the four ontogenetic stages as preserved in the Hayden Quarry silesaurid (GR 1072). (a) Eruption (fifth tooth): The tooth is actively replacing an old tooth, but is not yet functional. (b) Gomphosis (first tooth): the tooth is fully erupted, functional, and suspended in place by a periodontal ligament attached to the root cementum and alveolar bone. (c) Mineralization (third tooth): Tooth is partially ankylosed, in which the periodontal space is closed via the growth of alveolar bone in some, but not all regions around the tooth. (d) Ankylosis (third tooth): the periodontal space is completely closed via the continued growth of alveolar bone towards the cellular cementum (coating the tooth root), causing the complete closure of the periodontal space and the mineralization of the periodontal ligament within the alveolar bone and cementum

are simply pedomorphic relative to their therapsid ancestors in retaining teeth in a ligamentous stage of dental ontogeny. An equivalent process might also explain the origins of the dinosaur and crocodylian (and relatives) gomphosis. As is the case for mammals, the

gomphosis in dinosaurs and crocodylians may represent the retention of an early ontogenetic stage, in which alveolar bone does not completely enclose the periodontal ligament around the tooth. Our documentation of tooth attachment development in silesaurids is therefore a

promising model for the ancestral condition in the sister groups of dinosaurs and, possibly, crocodylians (see below).

Our findings on silesaurid dentition, combined with their debated phylogenetic position, has implications for the origins of the dinosaur gomphosis (Figure 17). Although usually considered the sister-group of Dinosauria (Figure 17a; Baron et al., 2017; Bittencourt

et al., 2015; Langer et al., 2010, 2017; Nesbitt et al., 2010, 2017; Nesbitt, 2011), an alternative hypothesis places silesaurids on the ornithischian lineage (Figure 17b; Cabreira et al., 2016; Ferigolo & Langer, 2007; Langer & Ferigolo, 2013; Müller & Garcia, 2020). If they are the sister taxon of Dinosauria, the delayed ankylosis of silesaurids implies that either delayed ankylosis is ancestral for Archosauria and the dinosaur and crocodylian

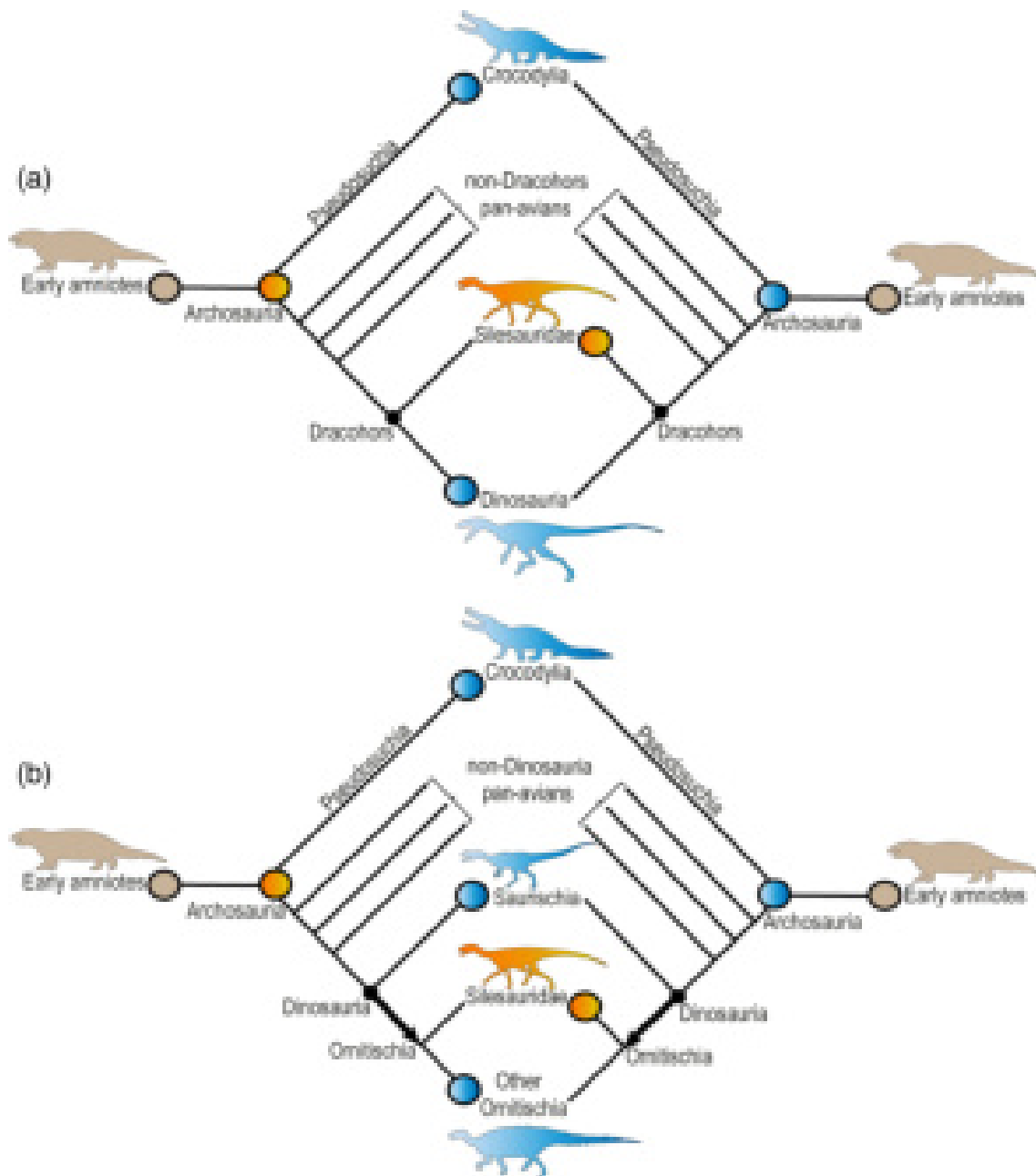


**FIGURE 17** Optimization of tooth attachment modes (permanent ankylosis = beige; delayed ankylosis = orange; permanent gomphosis = blue) in alternative phylogenetic positions of Silesauridae. (a) Silesauridae as sister-group of Dinosauria, with delayed ankylosis (left) or permanent gomphosis (right) as ancestral to Archosauria. (b) Silesauridae as ornithischians, with delayed ankylosis (left) or permanent gomphosis (right) as ancestral to Archosauria and Dinosauria. States and phylogenetic positions for each taxon from Nesbitt et al. (2010); Langer and Ferigolo (2013); Fong et al. (2016); LeBlanc et al. (2017); Chen et al. (2018)

permanent gomphosis arose convergently through a further delay and eventual truncation of the ankylosis stage (Figure 17a, left side), or that permanent gomphosis is ancestral for Archosauria (i.e., homologous between dinosaurs and crocodylians) and the silesaurid condition represents a synapomorphic reversal to the plesiomorphic state (Figure 17a, right side), in which the contact between cellular cementum and alveolar bone, once lost, can be again observed. The latter option represents the more traditional view (Edmund, 1960; Fong et al., 2016; LeBlanc et al., 2017; LeBlanc et al., 2018; Martz & Small, 2019; Nesbitt et al., 2010). Alternatively, if silesaurids are ornithischians, then either delayed ankylosis is plesiomorphic for Dinosauria and permanent gomphosis evolved convergently not only for dinosaurs and crocodylians, but also within dinosaurs, once in saurischians and again in ornithischians (Figure 17b, left side), or permanent gomphosis is ancestral for Dinosauria (i.e., homologous between ornithischians and saurischians) and delayed ankylosis represents a synapomorphic reversal of silesaurids (Figure 17b, right side). If silesaurids nest within Ornithischia, the latter scenario is overall more parsimonious, but given that the delayed ankylosis identified in silesaurids is likely to occur elsewhere in other non-dinosaur pan-avians, it may provide support for the nesting of silesaurids outside of Dinosauria. Further histological sampling is required not only to answer such questions, but also to more properly address the evolution of archosaur tooth attachment and test the homology of the permanent gomphosis of dinosaurs, crocodylians, and their relatives.

## 5 | CONCLUSIONS

Histological analysis of the tooth attachment system of various silesaurids challenges the concept that they possess a simple “ankylotheodont” dentition. Instead, tooth attachment in the group involves four phases of dental ontogeny: eruption, prolonged gomphosis, mineralization stage, and finally ankylosis. This explains why sections of silesaurid jaws reveal teeth in seemingly different states of tooth attachment. Our data demonstrate that ankylosis simply represents the last stage of tooth ontogeny in silesaurids, so that a broader study of dental tissues is necessary to shed light on the evolution of tooth attachment within dinosauromorphs. In fact, the “ankylotheodonty” to thecodonty transition appears to be the oversimplification of a more complex evolutionary history, and features involved in tooth attachment must be evaluated accurately when these are coded in archosaur phylogenies. Given the histological patterns we note

here for silesaurids, the permanent gomphosis of dinosaurs would represent one of the unique characteristics that define this intriguing group that thrived on Earth for more than 150 million years (Benton et al., 2014; Brusatte et al., 2008, 2010; Langer et al., 2010, 2013; Marsola, Ferreira, Langer, Button, & Butler, 2018).

## ACKNOWLEDGMENTS

We thank researchers, collection managers, and curators who provided access to the collections under their care, namely: Alex Downs, André Silveira, Cecilia Apaldetti, César Schultz, Claudio Revuelta, Fernando Abdala, Fernando Novas, Flávio Pretto, Gabriela Cisterna, Gretchen Gurtler, Leonardo Haerter, Leonardo Kerber, Martín Ezcurra, Michael Caldwell, Michelle Stocker, Pablo Ortiz, Pedro Hernández, Rodrigo Müller, Ricardo Martínez, Sergio Cabreira, and Vicki Yarborough. Thanks also to Gabriel Baréa for suggestions and improvement in the editing of the images.

## AUTHOR CONTRIBUTIONS

**Gabriel Mestriner:** Conceptualization; data curation; formal analysis; funding acquisition; investigation; methodology; project administration; resources; software; supervision; validation; visualization; writing-original draft; writing-review & editing. **Aaron LeBlanc:** Conceptualization; data curation; formal analysis; funding acquisition; investigation; methodology; project administration; resources; software; supervision; validation; visualization; writing-original draft; writing-review & editing. **Sterling Nesbitt:** Conceptualization; data curation; formal analysis; funding acquisition; investigation; methodology; project administration; resources; software; supervision; validation; visualization; writing-original draft; writing-review & editing. **Júlio Marsola:** Conceptualization; data curation; formal analysis; funding acquisition; investigation; methodology; project administration; resources; software; supervision; validation; visualization; writing-original draft; writing-review & editing. **Átila Da-Rosa:** Conceptualization; data curation; formal analysis; funding acquisition; investigation; methodology; project administration; resources; software; supervision; validation; visualization; writing-original draft; writing-review & editing. **Ana Ribeiro:** Conceptualization; data curation; formal analysis; funding acquisition; investigation; methodology; project administration; resources; software; supervision; validation; visualization; writing-original draft; writing-review & editing. **Jorge Ferigolo:**

Conceptualization; data curation; formal analysis; funding acquisition; investigation; methodology; project administration; resources; software; supervision; validation; visualization; writing-original draft; writing-review & editing. **Max Langer:** Conceptualization; data curation; formal analysis; funding acquisition; investigation; methodology; project administration; resources; software; supervision; validation; visualization; writing-original draft; writing-review & editing.

## ORCID

Gabriel Mestriner  <https://orcid.org/0000-0002-5542-1772>

Aaron LeBlanc  <https://orcid.org/0000-0002-2497-1296>

Sterling J. Nesbitt  <https://orcid.org/0000-0002-7017-1652>

Júlio C. A. Marsola  <https://orcid.org/0000-0001-5290-7884>

Átila Augusto Stock Da-Rosa  <https://orcid.org/0000-0003-4074-0794>

Max Langer  <https://orcid.org/0000-0003-1009-4605>

## REFERENCES

- Baron, M. G., Norman, D. B., & Barrett, P. M. (2017). A new hypothesis of dinosaur relationships and early dinosaur evolution. *Nature*, *543*(7646), 501–506.
- Benton, M. J., Forth, J., & Langer, M. C. (2014). Models for the rise of the dinosaurs. *Current Biology*, *24*(2), R87–R95.
- Benton, M. J., & Walker, A. D. (2011). *Saltopus*, a dinosauriform from the Upper Triassic of Scotland. *Earth and Environmental Science Transactions of the Royal Society of Edinburgh*, *101*(3–4), 285–299.
- Bertin, T. J., Thivichon-Prince, B., LeBlanc, A. R. H., Caldwell, M. W., & Viriot, L. (2018). Current perspectives on tooth implantation, attachment, and replacement in amniota. *Frontiers in Physiology*, *9*, 1630.
- Bittencourt, J. S., Arcucci, A. B., Marsicano, C. A., & Langer, M. C. (2015). Osteology of the Middle Triassic archosaur *Lewisuchus admixtus* Romer (Chañares Formation, Argentina), its inclusivity, and relationships amongst early dinosauromorphs. *Journal of Systematic Palaeontology*, *13*(3), 189–219.
- Bramble, K., LeBlanc, A. R. H., Lamoureux, D. O., Wosik, M., & Currie, P. J. (2017). Histological evidence for a dynamic dental battery in hadrosaurid dinosaurs. *Scientific Reports*, *7*, 15787.
- Breeden, B. T., Irmis, R. B., Nesbitt, S. J., Smith, N. D., & Turner, A. H. (2017). New silesaurid (Archosauria: Dinosauriformes) specimens from the Upper Triassic Chinle Formation of New Mexico and the phylogenetic relationships of *Eucoelophysis baldwini*. *Journal of Vertebrate Paleontology*, *37* (Suppl), 86.
- Brink, K. S., Reisz, R. R., LeBlanc, A. R. H., Chang, R. S., Lee, Y. C., Chiang, C. C., ... Evans, D. C. (2015). Developmental and evolutionary novelty in the serrated teeth of theropod dinosaurs. *Scientific Reports*, *5*, 12338.
- Brusatte, S. L., Benton, M. J., Ruta, M., & Lloyd, G. T. (2008). Superiority, competition, and opportunism in the evolutionary radiation of dinosaurs. *Science*, *321*(5895), 1485–1488.
- Brusatte, S. L., Nesbitt, S. J., Irmis, R. B., Butler, R. J., Benton, M. J., & Norell, M. A. (2010). The origin and early radiation of dinosaurs. *Earth-Science Reviews*, *101*(1–2), 68–100.
- Budney, L. A., Caldwell, M. W., & Albino, A. (2006). Tooth socket histology in the Cretaceous snake *Dinilysia*, with a review of amniote dental attachment tissues. *Journal of Vertebrate Paleontology*, *26*, 138–145.
- Cabreira, S. F., Kellner, A. W. A., Dias-da-Silva, S., da Silva, L. R., Bronzati, M., Marsola, J. C., ... Brodt, A. (2016). A unique Late Triassic dinosauriform assemblage reveals dinosaur ancestral anatomy and diet. *Current Biology*, *26*(22), 3090–3095.
- Caldwell, M. W. (2007). Ontogeny, anatomy and attachment of the dentition in mosasaurs (Mosasauridae: Squamata). *Zoological Journal of the Linnean Society*, *149*(4), 687–700.
- Caldwell, M. W., Budney, L. A., & Lamoureux, D. O. (2003). Histology of tooth attachment tissues in the Late Cretaceous mosasauroid *Platecarpus*. *Journal of Vertebrate Paleontology*, *23*, 622–630.
- Chen, J., LeBlanc, A. R. H., Jin, L., Huang, T., & Reisz, R. R. (2018). Tooth development, histology, and enamel microstructure in *Changchunsaurus parvus*: Implications for dental evolution in ornithomimid dinosaurs. *PLoS One*, *13*(11), e0205206.
- Dumont, M., Tafforeau, P., Bertin, T., Bhullar, B. A., Field, D., Schulp, A., ... Louchart, A. (2016). Synchrotron imaging of dentition provides insights into the biology of *Hesperornis* and *Ichthyornis*, the “last” toothed birds. *BMC Evolutionary Biology*, *16*(1), 178.
- Edmund, A. G. (1960). Tooth replacement phenomena in the lower vertebrates. *Royal Ontario Museum, Life Sciences Division, Contribution*, *52*, 1–190.
- Ezcurra, M. D. (2006). A review of the systematic position of the dinosauriform archosaur *Eucoelophysis baldwini* Sullivan & Lucas, 1999 from the Upper Triassic of New Mexico, USA. *Geodiversitas*, *28*(4), 649–684.
- Ezcurra, M. D. (2016). The phylogenetic relationships of basal archosauromorphs, with an emphasis on the systematics of proterosuchian archosauriforms. *PeerJ*, *4*, e1778.
- Ezcurra, M. D., Nesbitt, S. J., Fiorelli, L. E., & Desojo, J. B. (2019). New specimen sheds light on the anatomy and taxonomy of the early Late Triassic dinosauriforms from the Chañares Formation, NW Argentina. *The Anatomical Record*, *303*(5), 1393–1438.
- Ferigolo, J., & Langer, M. C. (2007). A Late Triassic dinosauriform from south Brazil and the origin of the ornithischian premaxillary bone. *Historical Biology*, *19*(1), 23–33.
- Fong, R. K., LeBlanc, A. R. H., Berman, D. S., & Reisz, R. R. (2016). Dental histology of *Coelophysis bauri* and the evolution of tooth attachment tissues in early dinosaurs: Dinosaur dental histology. *Journal of Morphology*, *277*, 916–924.
- García, R. A., & Zurriaguz, V. (2016). Histology of teeth and tooth attachment in titanosaurs (Dinosauria; Sauropoda). *Cretaceous Research*, *57*, 248–256.
- He, Y., Makovicky, P. J., Xu, X., & You, H. (2018). High-resolution computed tomographic analysis of tooth replacement pattern of the basal neoceratopsian *Liaoceratops yanzigouensis* informs ceratopsian dental evolution. *Scientific Reports*, *8*, 5870.
- Hendrichx, C., Mateus, O., & Araújo, R. (2015). A proposed terminology of theropod teeth (Dinosauria, Saurischia). *Journal of Vertebrate Paleontology*, *35*(5), e982797.
- Irmis, R. B., Nesbitt, S. J., Padian, K., Smith, N. D., Turner, A. H., Woody, D., & Downs, A. (2007). A late Triassic

- Dinosauriform assemblage from New Mexico and the rise of dinosaurs. *Science*, 317(5836), 358–361.
- Kammerer, C. F., Nesbitt, S. J., & Shubin, N. H. (2011). The first silesaurid dinosauriform from the Late Triassic of Morocco. *Acta Palaeontologica Polonica*, 57(2), 277–284.
- Kearney, M., & Rieppel, O. (2006). An investigation into the occurrence of plicidentine in the teeth of squamate reptiles. *Copeia*, 2006(3), 337–350.
- Kvam, T. (1960). The teeth of *Alligator mississippiensis* (Daud) VI. Periodontium. *Acta Odontologica Scandinavica*, 18, 67–82.
- Langer, M. C., Ezcurra, M. D., Bittencourt, J. S., & Novas, F. E. (2010). The origin and early evolution of dinosaurs. *Biological Reviews*, 85(1), 55–110.
- Langer, M. C., Ezcurra, M. D., Rauhut, O. W., Benton, M. J., Knoll, F., McPhee, B. W., ... Brusatte, S. L. (2017). Untangling the dinosaur family tree. *Nature*, 551(7678), E1–E3.
- Langer, M. C., & Ferigolo, J. (2013). The Late Triassic dinosauriform *Sacisaurus agudoensis* (Caturrita Formation; Rio Grande do Sul, Brazil): Anatomy and affinities. *Geological Society, London, Special Publications*, 379(1), 353–392.
- Langer, M. C., Nesbitt, S. J., Bittencourt, J. S., & Irmis, R. B. (2013). Non-dinosaurian dinosauriforms. *Geological Society, London, Special Publications*, 379(1), 157–186.
- Langer, M. C., Ramezani, J., & Da Rosa, A. S. (2018). U-Pb age constraints on dinosaur rise from South Brazil. *Gondwana Research*, 57, 133–140.
- LeBlanc, A. R. H., Brink, K. S., Cullen, T. M., & Reisz, R. R. (2017). Evolutionary implications of tooth attachment versus tooth implantation: A case study using dinosaur, crocodylian, and mammal teeth. *Journal of Vertebrate Paleontology*, 37, e1354006.
- LeBlanc, A. R. H., Brink, K. S., Whitney, M. R., Abdala, F., & Reisz, R. R. (2018). Dental ontogeny in extinct synapsids reveals a complex evolutionary history of the mammalian tooth attachment system. *Proceedings of the Royal Society B*, 285, 20181792.
- LeBlanc, A. R. H., Paparella, I., Lamoureux, D. O., Doschak, M. R., & Caldwell, M. W. (2020). Tooth attachment and pleurodonty implantation in lizards: Histology, development, and evolution. *Journal of Anatomy*, 238, 1156–1178. <https://doi.org/10.1111/joa.13371>
- LeBlanc, A. R. H., & Reisz, R. R. (2013). Periodontal ligament, cementum, and alveolar bone in the oldest herbivorous tetrapods, and their evolutionary significance. *PLoS One*, 8, e74697.
- LeBlanc, A. R. H., Reisz, R. R., Brink, K. S., & Abdala, F. (2016). Mineralized periodontia in extinct relatives of mammals shed light on the evolutionary history of mineral homeostasis in periodontal tissue maintenance. *Journal of Clinical Periodontology*, 43(4), 323–332.
- Luan, X., Walker, C., Dangaria, S., Ito, Y., Druzinsky, R., Jarosius, K., ... Rieppel, O. (2009). The mosasaur tooth attachment apparatus as paradigm for the evolution of the gnathostome periodontium. *Evolution & Development*, 11(3), 247–259.
- Marsola, J. C., Bittencourt, J. S., Da Rosa, A. S., Martinelli, A. G., Ribeiro, A. M., Ferigolo, J., & Langer, M. C. (2018). New sauropodomorph and cynodont remains from the late Triassic *Sacisaurus* site in Southern Brazil and its stratigraphic position in the Norian Caturrita Formation. *Acta Palaeontologica Polonica*, 63(4), 653–669.
- Marsola, J. C., Ferreira, G. S., Langer, M. C., Button, D. J., & Butler, R. J. (2018). Increases in sampling support the southern Gondwanan hypothesis for the origin of dinosaurs. *Palaeontology*, 62(3), 473–482.
- Martin, L. D., & Stewart, J. D. (1999). Implantation and replacement of bird teeth. *Smithsonian Contributions to Paleobiology*, 89, 295–300.
- Martz, J. W., & Small, B. J. (2019). Non-dinosaurian dinosauriforms from the Chinle Formation (Upper Triassic) of the Eagle Basin, northern Colorado: *Dromomeron romeri* (Lagerpetidae) and a new taxon, *Kwanasaurus williamparkeri* (Silesauridae). *PeerJ*, 7, e7551.
- Maxwell, E. E., Caldwell, M. W., & Lamoureux, D. O. (2011). The structure and phylogenetic distribution of amniote plicidentine. *Journal of Vertebrate Paleontology*, 31(3), 553–561.
- McIntosh, J. E., Anderton, X., Flores-De-Jacoby, L., Carlson, D. S., Shuler, C. F., & Diekwisch, T. G. H. (2002). *Caiman* periodontium as an intermediate between basal vertebrate ankylosis-type attachment and mammalian “true” periodontium. *Microscopy Research and Technique*, 59, 449–459.
- Melstrom, K. M., & Irmis, R. B. (2019). Repeated evolution of herbivorous crocodyliforms during the age of dinosaurs. *Current Biology*, 29, 2389–2395.
- Mestriner, G., Marsola, J. C., DaRosa, A. A. S., & Langer, M. C. (2018). First records of Silesauridae (Dinosauriformes) for the Brazilian Carniano (Santa Maria Formation, Superior Triassic). Abstract presented at the “Regional meeting of the Brazilian Paleontology Society”, Unicamp: <file:///C:/Users/User/Downloads/2018%20Paleo%20SP%20Campinas.pdf>.
- Miller, W. A. (1968). Periodontal attachment apparatus in the young *Caiman sclerops*. *Archives of Oral Biology*, 13, 735–743.
- Müller, R. T., & Garcia, M. S. (2020). A paraphyletic ‘Silesauridae’ as an alternative hypothesis for the initial radiation of ornithischian dinosaurs. *Biology Letters*, 16, 20200417.
- Nanci, A. (2013). *Ten Cate's oral histology: Development, structure, and function*. Amsterdam: Elsevier 379 pp.
- Nesbitt, S. J. (2011). The early evolution of archosaurs: Relationships and the origin of major clades. *Bulletin of the American Museum of Natural History*, 2011(352), 1–292.
- Nesbitt, S. J., Butler, R. J., Ezcurra, M. D., Barrett, P. M., Stocker, M. R., Angielczyk, K. D., ... Charig, A. J. (2017). The earliest bird-line archosaurs and the assembly of the dinosaur body plan. *Nature*, 544(7651), 484–487.
- Nesbitt, S. J., Langer, M. C., & Ezcurra, M. D. (2020). The anatomy of *Asilisaurus kongwe*, a dinosauriform from the Lifua Member of the Manda Beds (~ Middle Triassic) of Africa. *The Anatomical Record*, 303(4), 813–873.
- Nesbitt, S. J., Sidor, C. A., Irmis, R. B., Angielczyk, K. D., Smith, R. M., & Tsuji, L. A. (2010). Ecologically distinct dinosaurian sister group shows early diversification of Ornithodira. *Nature*, 464(7285), 95–98.
- Osborn, J. W. (1984). From reptile to mammal: Evolutionary considerations of the dentition with emphasis on tooth attachment. *Symposia of the Zoological Society of London*, 52, 549–574.
- Peacock, B. R., Steyer, J. S., Tabor, N. J., & Smith, R. M. (2018). Updated geology and vertebrate paleontology of the Triassic Ntawere Formation of Northeastern Zambia, with special emphasis on the archosauromorphs. *Journal of Vertebrate Paleontology*, 37(Suppl. 1), 8–38.

- Peyer, B. (1968). *Comparative odontology* (pp. 80–110). Chicago: The University of Chicago Press.
- Pretto, R. A., Cabreira, S. F., & Schultz, C. L. (2014). Tooth microstructure of the Early Permian aquatic predator *Stereosternum tumidum*. *Acta Palaeontologica Polonica*, *59*, 125–133.
- Qvarnström, M., Wernström, J. V., Piechowski, R., Talanda, M., Ahlberg, P. E., & Niedzwiedzki, G. (2019). Beetle-bearing coprolites possibly reveal the diet of a Late Triassic dinosauriform. *Royal Society Open Science*, *6*(3), 181042.
- Reid, R. E. H. (1996). Bone histology of the Cleveland-Lloyd dinosaurs and of dinosaurs in general, part 1: Introduction: Introduction to bone tissues. *Brigham Young University, Geological Studies*, *41*, 25–71.
- Richman, J. M., & Handrigan, G. R. (2011). Reptilian tooth development. *Genesis*, *49*(4), 247–260.
- Saffar, J. L., Lasfargues, J. J., & Cherruau, M. (1997). Alveolar bone and the alveolar process: The socket that is never stable. *Periodontology*, *2000*(13), 76–90.
- Sassoon, J., Foffa, D., & Marek, R. (2015). Dental ontogeny and replacement in Pliosauridae. *Royal Society Open Science*, *2*(11), 150384.
- Snyder, A. J., LeBlanc, A. R. H., Jun, C., Bevitt, J. J., & Reisz, R. R. (2020). Thecodont tooth attachment and replacement in bolosaurid parareptiles. *PeerJ*, *8*, e9168.
- Sullivan, R. M., & Lucas, S. G. (1999). *Eucoelophysis baldwini* a new theropod dinosaur from the Upper Triassic of New Mexico, and the status of the original types of *Coelophysis*. *Journal of Vertebrate Paleontology*, *19*(1), 81–90.
- Tomes, C. S. (1874). Studies upon the attachment of teeth. *Transactions of the Odontological Society of Great Britain*, *7*, 41–58.
- Wang, C. C., Song, Y. F., Song, S. R., Ji, Q., Chiang, C. C., Meng, Q., ... Reisz, R. R. (2015). Evolution and function of dinosaur teeth at ultramicrostructural level revealed using synchrotron transmission X-ray microscopy. *Scientific Reports*, *5*, 15202.
- Wu, P., Wu, X., Jiang, T. X., Elsey, R. M., Temple, B. L., Divers, S. J., ... Chuong, C. M. (2013). Specialized stem cell niche enables repetitive renewal of alligator teeth. *Proceedings of the National Academy of Sciences*, *110*(22), E2009–E2018.
- Zaher, H., & Rieppel, O. (1999). Tooth implantation and replacement in squamates, with special reference to mosasaur lizards and snakes. *American Museum Novitates*, *3271*, 1–19.

## SUPPORTING INFORMATION

Additional supporting information may be found online in the Supporting Information section at the end of this article.

**How to cite this article:** Mestriner, G., LeBlanc, A., Nesbitt, S. J., Marsola, J. C. A., Irmis, R. B., Da-Rosa, Átila Augusto Stock, Ribeiro, A. M., Ferigolo, J., & Langer, M. (2021). Histological analysis of ankylothecondonty in Silesauridae (Archosauria: Dinosauriformes) and its implications for the evolution of dinosaur tooth attachment. *The Anatomical Record*, 1–31. <https://doi.org/10.1002/ar.24679>